[AMERICAN JOURNAL OF SCIENCE, VOL. 279, MARCH, 1979, P. 225-271]

American Journal of Science

MARCH 1979

SEQUENCE OF STRUCTURAL STAGES OF THE ALLEGHANY OROGENY, AT THE BEAR VALLEY STRIP MINE, SHAMOKIN, PENNSYLVANIA

RICHARD P. NICKELSEN

Department of Geology and Geography,
Bucknell University, Lewisburg, Pennsylvania 17837

ABSTRACT. All recognized structural stages of the Alleghany orogeny in the northern Valley and Ridge Province are visible in a large mine of Pennsylvanian-age anthracite, the Bear Valley Strip Mine near Shamokin, Pa. This unique, three-dimensional exposure shows the following sequence of structural events: (I) extension jointing in coals prior to the Alleghany orogeny; (II) extension jointing in sandstones and ironstones, the first Alleghany event; (III) spaced cleavage in shales and small-scale (wave length 10 cm) folding in ironstone beds (pressure solution associated with cleavage caused offset of earlier stage II extension joints); (IV) conjugate wrench faulting and thrusting (wedging) as σ_2 and σ_3 locally traded orientations (cleavage and small folds of III are dragged against wrench faults, thus establishing sequence); (V) large-scale (wave length 65 m or larger) kink folding, which deformed all previous structures; (VI) extension in the outer arc of bent sandstone layers creating strike grabens and transverse grabens, some following earlier wrench faults.

Because all structural stages are superimposed at one place, progressive deformation and the relative time of formation of joints, rock cleavage, minor folds, faults, and major folds can be proven. Thus, extension jointing occurred first and recurred in different directions during II, IV, and VI. Cleavage and small folds were initiated in horizontal beds before wedging and wrench faulting and were deformed during IV and V. The present, distorted attitude of early strain axes reveals the rotations they experienced during later stages of deformation.

Microscopically, rock cleavage appears as close-spaced crenulations or clay-carbon partings. The two-dimensional ratio of principal elongations associated with cleavage has been determined at several localities.

INTRODUCTION

The abandoned Bear Valley Strip Mine in the western part of the Middle Anthracite field is a remarkable outcrop which displays most of the structural features of the Appalachian Valley and Ridge Province in Pennsylvania (pl. 1-A, -B). This important locality may provide a new insight into the structural development of the northern Valley and Ridge Province, a topic that has undergone considerable recent revision.

During the last 15 yrs, there have been three major changes in classical views of the structure of this province: (1) Major subsurface thrusts were found, and the thin-skinned nature of the deformation was established (Gwinn, 1964, 1970; Rodgers, 1970; Wood and Bergin, 1970), thus extending northward into Pennsylvania a style of deformation long recognized in the southern Valley and Ridge Province. (2) A "kink" geometry, rather than concentric fold profiles, was shown to exist in many folds of all sizes (Faill, 1969, 1973). (3) Pre-folding, penetrative deformation was

PLATE 1

Overview of Bear Valley Strip Mine

A. View toward the southeast corner over whaleback anticline. Syncline on east wall is on left, south wall on right.

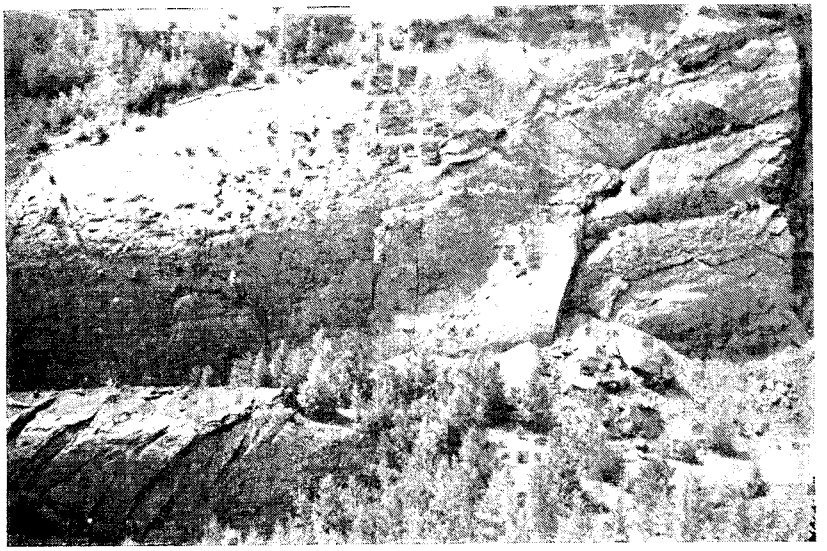

B. View toward the south wall and southwest corner over the whaleback anticline. Compare with figure 6.

documented throughout the Valley and Ridge and westward into the Appalachian Plateau by measurement of deformed fossils, mudcrack polygons, reduction spots, and twinned calcite grains (Nickelsen, 1966, 1972; Faill and Nickelsen, 1973; Geiser, 1974; Groshong, 1975; Engelder and Engelder, 1977; Perry, 1975).

The outcrops in the Bear Valley Strip Mine provide evidence for what may be an additional step in this group of revisions, the recognition of a progressive sequence of structural stages throughout a single orogeny. This has been touched upon previously by Cloos (1961), Arndt and Wood (1960), Wood, Trexler, and Kehn (1969), and Perry (1975) but awaits further documentation at exposures where geometric relationships between structural elements are visible in three dimensions.

The mine is owned by the Reading Anthracite Company, which has tolerated its educational use by many institutions. It is located 4.42 km southwest of Shamokin, Pa. on the south limb of the first order syncline making up the western part of the Middle Anthracite Field (fig. 1). Strip mining was terminated in 1952, and subsequent weathering has enhanced many geologic features. The geologically most interesting part of the mine measures 300 m (east-west) by 120 m (north-south) and is approx 75 percent bare bedrock exposure.

Geologic maps covering the area were published by Arndt, Danilchuk, and Wood (1963) and republished in different formats by Arndt, Wood, and Schryver (1973). Unfortunately, both these maps were printed on a topographic base prepared prior to 1952 for the United States Geological Survey 15-min topographic map series (Shamokin 15″ quad.), and neither map correctly depicts the present topography of the mine area. Accurate portrayal of the topography and roads appears on the Shamokin 7½″ quadrangle (1969), at approx 40° 45′ 50″ north and 76° 35′ 45″ west. Localities within the mine referred to in the following

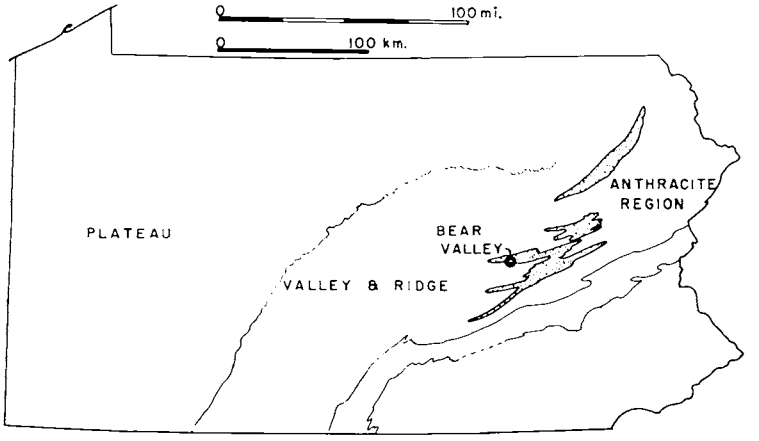

Fig. 1. Index map of Pennsylvania

description may be located on the geologic map (fig. 2, opposite p. 264). The crest and north and south limbs of the whaleback anticline have been marked on the outcrop with paint at 30.4 m (100 ft) intervals from west to east with numbers: 0, 1, 2, 3, 4.

STRATIGRAPHY

The stratigraphic sequence in the Bear Valley Strip Mine is part of the Llewellyn Formation, commonly referred to as post-Pottsville rocks. It consists of conglomeratic sandstone, sandstone, mudstone, anthracite or semi-anthracite, and interbedded clayey or silty shale and sandstone or siltstone, ascending in rudely cyclic sequences. At the east end of the mine, the vertical wall shows a syncline in the interbedded shales and sandstones of the upper part of the Mammoth Coal Zone cycle, overlain by the thick sandstone of the next cycle (either the Top Split #9 coal cycle or the Four Foot #9½ coal cycle; Arndt, Danilchuk, and Wood, 1963, sheet 2, column 7).

Within the mine the Mammoth Coal Zone (coals numbered 8, 8½, and 9) was removed, and the south wall shows the floor of the Mammoth Bottom Split Coal Bed (#8) which is "carbonaceous claystone that in places contains many elliptical concretions of siltstone and iron carbonates" (Arndt, Danilchuk, and Wood, 1963, sheet 2). The ironstone concretions are less obvious on the northernmost anticline except at the northeast end above the "lake" and just east of the entrance road, and it appears that the mine was not developed down to the level of the #8 coal in much of this area. Essentially then, the two anticlines and synclines of the mine have been stripped to the level of the sandstone or sandstones beneath or within the Mammoth Coal Zone. The concretionary sandstone beneath the #8 coal is the surface exposed throughout most of the mine: on the south wall, the whaleback anticline, and part of the north anticline. The sandstone was sampled in the cut at the west end of the whaleback anticline. Point counts of three thin sections revealed the following range of composition:

Quartz	63 to 77 percent
Labile rock fragments	6 to 17 percent
Matrix	11 to 15 percent

This classifies the sandstone as a sublitharenite (Pettijohn, 1975, p. 211), and its appearance is similar to the photomicrograph of a Pottsville Formation sandstone pictured in Pettijohn, Potter, and Siever (1972, figs. 6-7, p. 193).

STRUCTURAL GEOLOGY

Introduction.—This one large exposure in the Bear Valley Strip Mine contains virtually all the structural elements and stages of deformation that are recognized in the Valley and Ridge Province. It can serve as a type area for exemplifying the style, mechanics, and stages of structural development of this part of the Applachians and provide a datum

for comparison with other deformed areas in the Appalachians and elsewhere.

Structural elements that may be observed are joints, spaced cleavage, and thrust, wrench, and normal faults as well as lineations including minor folds, cleavage-bedding intersections, and slickenlines (Fleuty, 1975) on slickensided surfaces. Folds of third-order size (Nickelsen, 1963) are exposed in three dimensions, and, at the east wall, a vertical section reveals fold disharmony between two litho-tectonic units. A sequence of deformational stages can be observed which partially supports Arndt and Wood's (1960) and Wood, Trexler, and Kehn's (1969, p. 113) interpretation of the progressive sequence in the western part of the Southern Anthracite Field. There is evidence of early jointing, later spaced and/or crenulation cleavage, and slightly later thrust-wrench systems of faulting, followed by kink-band folding, which rotated cleavage, joints, and earlier thrust-wrench fault systems. It is also apparent that as folding progressed, steep upthrusts were generated in fold cores, and the upper surfaces of beds in anticlines were stretched both parallel and perpendicular to hinges, resulting in both strike and transverse grabens.

The structure will be described by reporting the six overlapping structural stages that can be differentiated and identifying the structural elements within each (table 1). Since all but one of the structural stages are a product of one (Alleghany) orogeny, the different stages are thought to be due to: (1) change in the mechanical properties of sedimentary rocks during progressive deformation and diagenesis, (2) progressive rotation of early strain axes during later episodes of strain, (3) increase in stress difference throughout earlier episodes of deformation, (4) exchanging positions of σ_2 and σ_3 at several times during deformation. The result has been a progressive change in the dominant deformation mechanism from extension fracturing to pressure solution and small-scale, intrabed folding, to thrust and wrench faulting, to buckling with asso-

TABLE 1
Sequence of structural stages

Stage		Event
I		Pre-Alleghany jointing — coal
II	↑	Extension jointing — ironstone, sandstone
III	ALLEGHANY	Cleavage, small scale folding
IV		Conjugate wrench and thrust faulting
V		Large scale folding, jointing
VI	↓	Fold-generated grabens and upthrusts

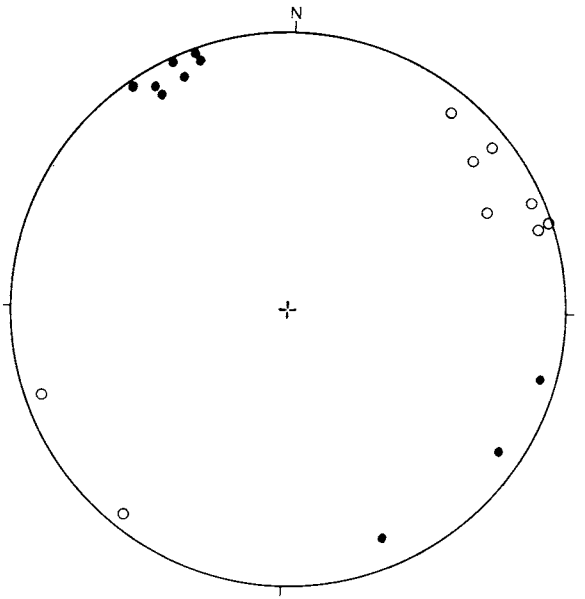

Fig. 3. Equal-area projection: poles to joints in coal, rotated around the strike of bedding to prefolding orientation. Solid circles — systematic joints; Open circles — nonsystematic joints.

ciated extension and compression above and below neutral surfaces of bent members.

Stage I: Pre-Alleghany northeast-striking extension joints in coal.— At several localities on the north anticline and at the southeast corner, remnants of the Mammoth Bottom Split Coal or coaly partings in sandstones show a well-developed fundamental joint system (Nickelsen and Hough, 1967, p. 615) consisting of orthogonal systematic and non-systematic joint sets. These joints are spaced at intervals of several millimeters. Figure 3 is a projection[1] of all joints in coal, rotated with bedding,[2] to show the inferred orientation prior to folding. Two features are significant:

1. The systematic joints of this fundamental system in coals trend Az 50 to 70 (poles plot between 320 and 340), whereas systematic joints of Alleghany age in other rock types trend northwest.
2. Joints in coal are not symmetrical with any of the later structural stages recognized in the mine, but they do parallel the systematic joints at the eastern end of the arc of Set 1 joints in coal described on the Appalachian Plateau, 60 km to the northwest (Nickelsen and Hough, 1967, p. 619, pl. 3).

[1] All projections in this article are lower-hemisphere Schmidt-net equal-area projections.

[2] "Rotated with bedding" means rotated around the strike of bedding at the same angle and direction needed to return bedding to horizontal.

PLATE 2

Joints

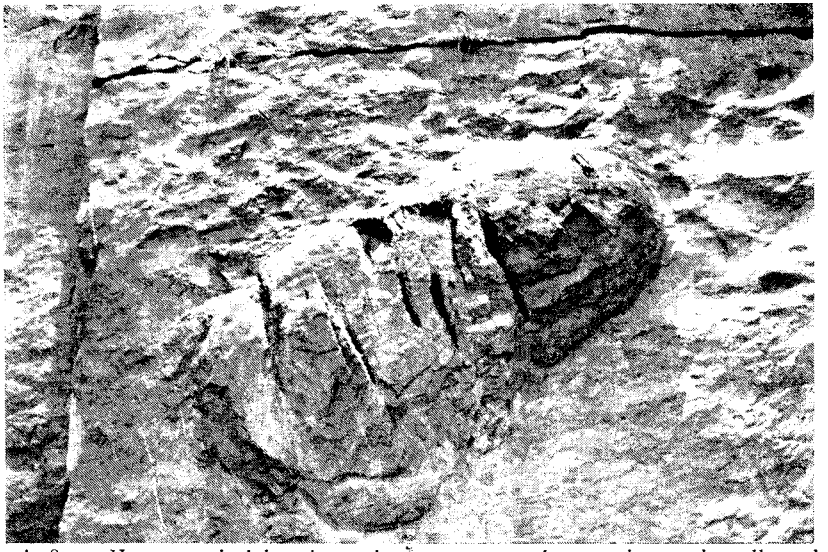

A. Stage II systematic joints in an ironstone concretion on the south wall at the center of plate 1-A. The vertical plane on the left is a stage IV left-lateral wrench fault. The horizontal plane near the top is a stage IV extension joint.

B. Cumulative joint pattern resulting from stages II, IV, and VI extension fracturing. Photographed in northeast corner.

As previously suggested for the Appalachian Plateau (Nickelsen and Hough, 1967, p. 626), these joints in coal are pre-Alleghany in age, related to the repeated doming in north-central Pennsylvania which has been documented by Williams and Bragonier (1974, p. 134-143). Because of low stress differences or differing mechanical properties of rocks at the time they were formed, this early period of epeirogenic deformation produced only extension joints in coals. They were subsequently overprinted by structures related to northwesterly compression during the stages of the Alleghany orogeny described below.

Stage II: Early Alleghany, northwest-striking systematic joints in ironstone and sandstone.—Ironstone, sandstone, or shale all contain en-echelon zones of quartz-filled extension joints belonging to this episode of deformation, but the joints attain their best development in ironstone nodules (see pl. 2-A). Though commonly only one set is present, two sets of these joints intersecting at approx 30° may be seen at places in the ironstones in the southwest and northwest corner, in sandstones on the west end of the whaleback anticline, and in the ironstones north of the lake in the northeast corner (fig. 2). Non-systematic joints orthogonal to these more prominent systematic joints are not common. Systematic joints such as those illustrated in plate 2-A are interpreted as extension fractures formed early in the deformation history as fluid pressure or the stress difference associated with the Alleghany orogeny increased. Two different sets of systematic joints formed as the principal stress axes rotated in the plane of the still horizontal bedding. Small-scale stage III folds and bedding-cleavage intersections are commonly oriented perpendicular or at a large angle to these stage II joints and are considered slightly later than the joints for reasons discussed below. Later stages of deformation have changed the orientation of early Alleghany joints as shown in the interpretive strain map of figure 12. In places where two acutely intersecting systematic joints occur, they have both been rotated by the later strain while maintaining their 30-degree angle of intersection.

Plate 2-B, depicting a bedding plane of sandstone in the northeast corner, shows vertical extension joints of stage II and other joints formed during stages IV and VI. The cumulative joint pattern illustrated in plate 2-A and -B will be discussed below under stage VI.

Stage III: Small-scale folding and spaced cleavage.—Small-scale folds and bedding-cleavage (S_0/S_1) intersections rarely parallel the hinge of the larger folds in the mine. In most cases, when rotated with bedding they strike in a more northerly direction than the hinges of large folds (fig. 4). I believe they were initiated in horizontal beds and later folded and rotated to their present attitude by the faults of stage IV and the large folds of stage V. Stage III folding and cleavage show interesting sequential relationships with other stages of deformation. Stage II joints are commonly nearly perpendicular to the minor folds and bedding-cleavage intersections of stage III, but in places where both sets of extension joints are present, one set cannot be perpendicular to bedding-cleavage intersections. This oblique joint set is offset at bedding-

cleavage intersections in the hinges of tight minor folds in ironstone, the offset originating from volume loss due to pressure solution perpendicular to the cleavage plane, one of the dominant processes forming cleavage (pl. 3-A). This observation proves that cleavage and the tighter minor fold hinges postdate at least some of the stage II joints. Further, cleavage planes, bedding-cleavage intersections, and small-scale fold hinges are dragged against wrench faults of stage IV and are rotated by the folding of stage V, thus proving that cleavage was initiated prior to both these events. Plate 3-B is a bedding-plane view of a conjugate pair of stage IV wrench faults which deform minor folds and bedding-cleavage intersections with right-lateral and left-lateral drag. A close-up of the left-lateral wrench fault (fig. 5) shows not only drag of folds and cleavage-bedding intersections but also en-echelon extension joints perpendicular to the long axis of the strain ellipse that can be inferred from the sense of drag.

Slickenlines formed by differential slip between ironstone concretions and their matrix are largely confined to down-dip orientations on the bedding plane. Differential slip occurs because shale, mudstone, or sandstone of the matrix undergoes either volume loss due to pressure solution or layer-parallel shortening caused by crenulation and layer-parallel packing, whereas non-ductile ironstone concretions remain volume constant and unshortened. Where best exposed along the south wall

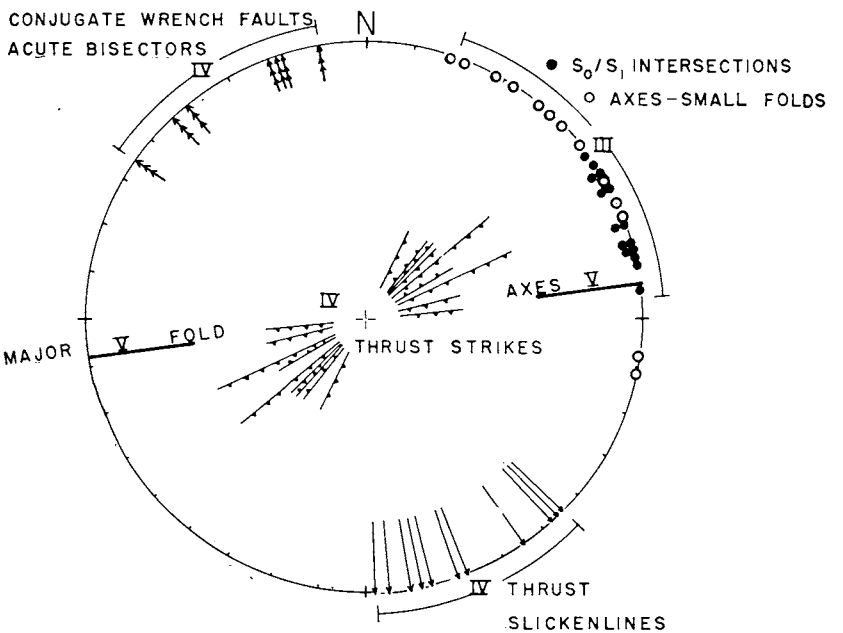

Fig. 4. Equal-area projection: stage III and IV structural elements compared to orientation of stage V fold hinge. Prior to plotting stage III and IV elements were rotated around strike of bedding to their prefolding orientation.

PLATE 3

Relationship of cleavage to joints and wrench faults

A. View of bedding plane where stage II quartz-filled extension joints are offset against bedding-cleavage intersections because cleavage is a plane of pressure solution. Joints trend north-south, cleavage east-west. Coin diameter is 1.7 cm.

and on the north limb of the whaleback anticline at #1, slickenlines parallel the bedding traces of stage II extension joints and are perpendicular to stage III bedding-cleavage intersections. They parallel the strain axes formed during stages II and III and are thought to be of similar relative age. Where neither stage II joints nor stage III bedding-cleavage intersections are visible, these slickenlines have been used to track the orientation of the minimum axis of the strain ellipse of those stages on the bedding plane (fig. 12).

Stage IV: Thrust and wrench faulting.—Conjugate pairs of wrench faults and thrust faults showing overthrusting toward either the northwest or the southeast are well exposed on the south wall (pls. 1-B, 7-A; fig. 6) and the whaleback anticline. All wrench and thrust faults have been folded by stage V folds and thus originated earlier, but some wrench faults definitely continued growing into the period of large-scale folding. Within stage IV it is generally not possible to separate sub-stages of wrench faulting from thrusting. The two classes of faults apparently operated either simultaneously in adjacent subareas or in an alternating manner in one area throughout deformation, as σ_2 and σ_3 switched positions either in space or time. The relative slip sense on wrench faults viewed in the bedding plane is established by the mutual rela-

PLATE 3 (continued)

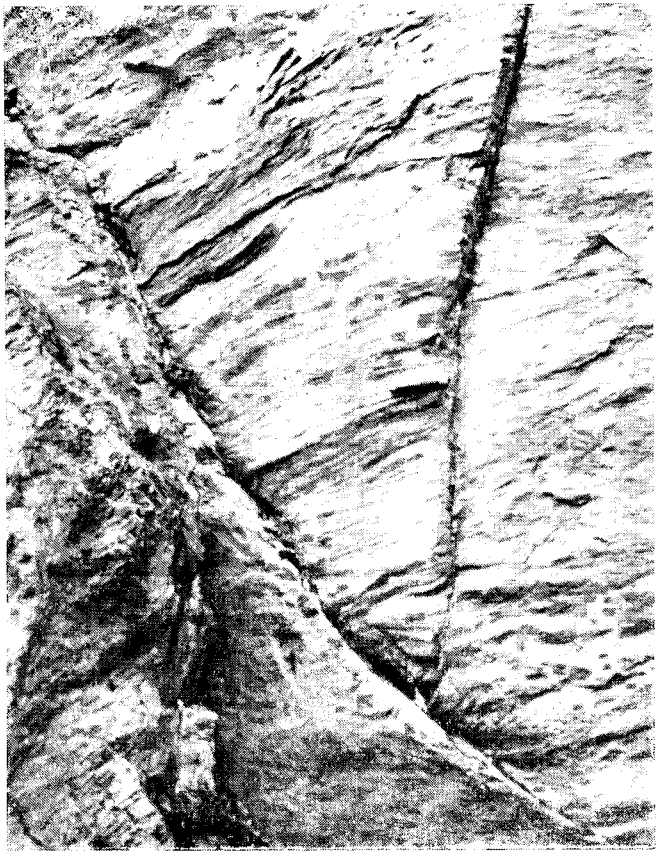

B. Conjugate right-lateral and left-lateral wrench faults on the bedding plane of the south wall near #0. Bedding-cleavage intersections and minor folds are dragged against wrench faults. Figure 6 is a close-up drawing of the left-lateral wrench fault.

tionships of faults, slickenlines indicating net-slip directions, and displacement of bedding (pl. 4-A), by offset ironstone concretions (pl. 4-B), and by wrench fault-slickenline-fold relationships (pl. 5-A and -B).

In different parts of the mine, either wrench faults or thrust faults may be dominant in size and frequency. Wrench faults penetrate the interior of thrust blocks in complex arrays of left- and right-lateral shears, as shown in the south wall thrust between #0 and #1. Wrench faults are most apparent as a number of steeply-dipping faults on the south wall near the southwest corner, at #2 on the south wall, in the southeast corner, and in the north syncline at #2. At #2 on the south wall and in the southwest corner, the dominant conjugate wrench faults are accompanied by minor wedge thrusts (Cloos, 1961). Slickenlines on the wedge thrusts approximately bisect the acute angle between the wrench faults as shown in plate 6-A. The acute angle between conjugate

right- and left-lateral wrench faults (when viewed in the bedding plane) ranges from 20° to 45° with a mean angle of 32.7°, based upon 15 measurements of the angle from throughout the mine. Either the left-lateral fault (pl. 6-A) or the right-lateral fault (pls. 3-B, 5-A) may dominate or show last movement in any pair of conjugate faults.

Between #1 on the south wall and the southwest corner of the mine, there are two differently oriented conjugate wrench-fault pairs (pls. 1-B, 6-B) labelled IVA and IVB on the interpretative drawing (fig. 6). At the southwest corner the right-lateral fault set of the conjugate wrench fault system labelled IVA is strongly developed (pl. 6-B). Both the right-lateral faults and the rare left-lateral faults of this system dip west, and the acute bisector of these faults rakes 50° from the west

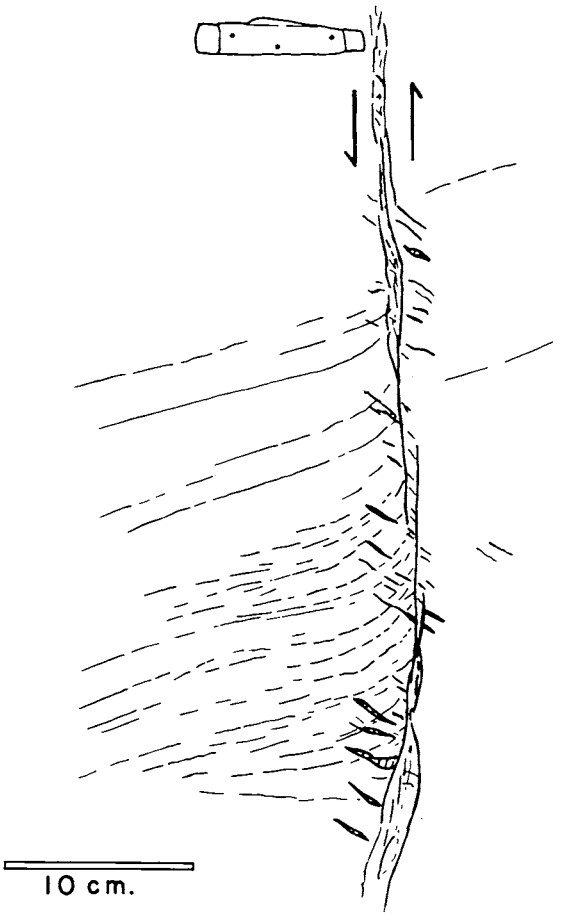

Fig. 5. Close up of left-lateral wrench fault of plate 3-B. Note left-lateral drag of bedding-cleavage intersections and minor folds. The slip sense and relative age of cleavage and faulting are also indicated by open gash joints in the fault zone.

in the bedding plane (fig. 6). Small wedge thrusts at the southwest corner related to this IVA system of wrench faults have slickenlines that also rake 60° from the west in the fault plane. The acute bisector of the conjugate wrench faults and the thrust slickenlines both define the IVA minimum axis of strain. The IVB conjugate wrench-fault system is represented only by the vertical left-lateral fault at the southwest corner, but toward the east, especially between #1 and #2, the west-dipping right-lateral faults are equally well-developed (pl. 4-A). The acute bisector of this IVB conjugate wrench-fault system rakes 76° to 78° from the west, and slickenlines on associated wedge thrusts at #2 on the south wall also rake 74° from the west (pl. 6-A; fig. 6). Thus, in one interpretation, the minimum axis of the strain ellipse during stage IVB had rotated clockwise approx 15° or 20° from its position during stage IVA, resulting in an over-printing of the two differently oriented conjugate wrench-fault systems. The relative age of the stage IVA and IVB wrench-fault conjugate systems is based upon the truncation of IVA right-lateral faults by a large IVB left-lateral fault at the southwest corner (pl. 6-B; fig. 6). Alternatively, two domains of different stress orientation, separated by the large IVB left-lateral faults of plate 6-B but operating simultaneously, could produce the same geometric relationship (William Chapple, personal commun., 1977).

The IVB wrench fault system is associated with the thrust fault on the south wall between #1 and 100′ west of #0 (pl. 1-B; fig. 6). The thrust block probably originally extended farther west and has been removed by mining. Wrench faults of the IVB system occur both within and beneath the thrust plate at different places along the south wall.

In contrast to the overprinting in the southwest corner, the IVA and IVB conjugate wrench-faults systems appear to grade into one another at the southeast corner of the mine where there is an abrupt change of 25° in the attitude of the right-lateral wrench fault visible on the lower part of the huge-bedding-plane exposure shown in plate 5-A. This observation supports the view that the IVA and IVB conjugate wrench-fault systems are different local domains in space rather than time.

Thrust faults vary in size and net slip from small intra-bed "wedge" thrusts (pls. 6-A, 7-A) to thrusts that cut completely through the basal sandstone (figs. 6, 7; pl. 1-B). When rotated with bedding to their pre-folding attitude, a majority of the thrust faults of all sizes strike north of the trend of stage V folds (fig. 4). This is also apparent from the attitude of thrust-fault traces on limbs of folds at a number of places. On north-dipping limbs for example, the trace of the thrust fault on the south wall between #0 and #1 plunges irregularly to the east (pl. 1-B; fig. 6) as does the trace of the thrust on the north limb of the whaleback anticline between #3 and #4 (pl. 7-B; fig. 7) and the thrust high on the south wall 90 m west of the southeast corner. On south-dipping limbs the traces of thrust faults plunge southwest as at #4 on the north anticline. When slickenlines on thrust faults are rotated with bedding

PLATE 4

Wrench faults on the south wall

A. South wall from #0 to #2, showing conjugate wrench faults and horizontal joints. Left-lateral wrench faults are vertical. Right-lateral wrench faults dip 60° right (west). Both sets of wrench faults have been bent by stage V folding with no destruction or renewed bedding separation. Horizontal joints are stage VI extension joints.

they plot in the southwest quadrant grouped around az 155°, *not* symmetrical to the hinge of stage V folds but perpendicular to the traces of thrust faults (fig. 4). On the basis of the attitude of thrust traces on bedding and the slickenlines on thrust planes, it would appear that the stage V folds were superimposed later at an angle of 15° or 20° upon stage IV thrusts. The most obvious exception to this generalization is the thrust between #0 and #2 on the north limb of the whaleback anticline with a trace plunging west (fig. 7.) Since other early strain markers (stage IV conjugate wrench faults, bedding-cleavage intersections, stage II extension joints, and down-dip slickenlines on concretions) maintain their mutual orientation here, it is concluded that all have been rotated, during stage V folding, more complexly than elsewhere in the mine. In addition to the rotation around the strike of bedding which is recognized everywhere, the area between #0 and #2 on the north limb of the whaleback has apparently been rotated clockwise more than 30° around the perpendicular to bedding. The latter rotation resulted from the west plunge of the whaleback anticline, but the mechanism of rotation is not known.

Rotation of stage IV thrust and wrench faults and slickenlines by stage V folding is well documented in the accessible fourth-order fold in the north syncline between #1 and #2 (fig. 2; pl. 8). Figure 8 shows data measured on and adjacent to the left-lateral wrench fault visible, with slickenlines, to the left of the anticlinal crest in plate 8-A and to

PLATE 4 (continued)

B. Conjugate wrench faults on the south wall near #2 at the lower left corner of (A). The vertical, left-lateral wrench fault in the left center offsets two ironstone concretions.

the right of the hammer in plate 8-B. Poles of bedding define a π pole and hinge that is located 50° from the poles to faults. The poles of all possible wrench fault segments that are 50° from the π pole were plotted as a small-circle trace on figure 8. Field-measured poles of different segments of the folded wrench fault fall on or near the small circle, thus proving that the wrench fault preceded folding and was rotated to its present attitude during stage V folding. Likewise, the 70° spread in the orientation of slickenlines on the wrench fault must be explained by folding the originally parallel slickenlines. The attitude of the small thrust visible on the bedding plane above the hammer in plate 8-A also requires stage IV thrusting preceding stage V folding.

Slickenlines on most wrench faults of the south wall are parallel or nearly parallel to bedding-fault intersections and have been rotated with bedding during stage V folding, thus indicating that most stage IV

PLATE 5

Wrench faults in the southeast corner

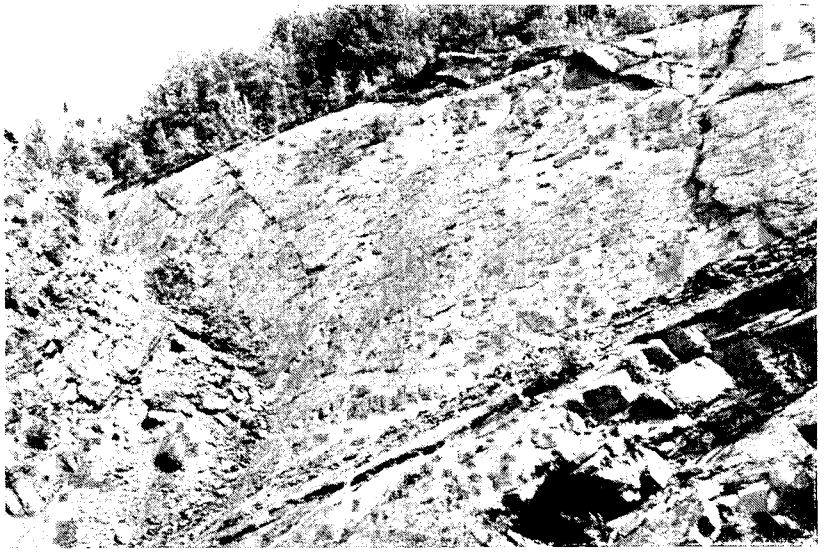

A. The large, warped, bedding surface of the southeast corner, which shows traces of conjugate wrench faults. Traces of left-lateral wrench faults plunge down the dip of bedding, while traces of right-lateral wrench faults plunge toward the observer. Note the small fold truncated by a right-lateral wrench fault in the upper right.

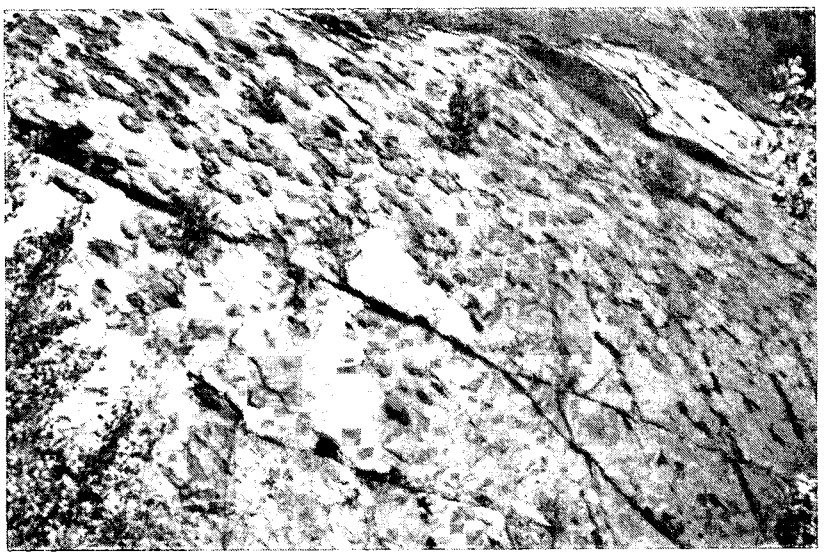

B. Bedding surface of the southeast corner viewed toward the southwest. Traces of right-lateral wrench faults plunge toward the lower right; left-lateral fault traces are steeper. The fold terminating against the slickenlined wrench fault in the upper right proves that right-lateral slip has occurred.

PLATE 6

Wrench fault-thrust relationship

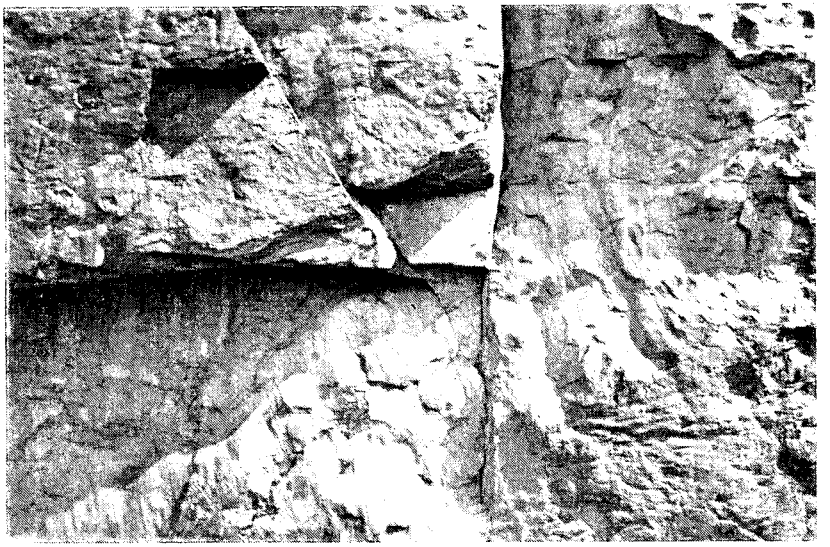

A. Conjugate wrench faults and an associated thrust fault on the south wall near #2. Slickenlines on the thrust fault bisect the acute angle between the wrench faults. Horizontal fractures are stage VI extension joints.

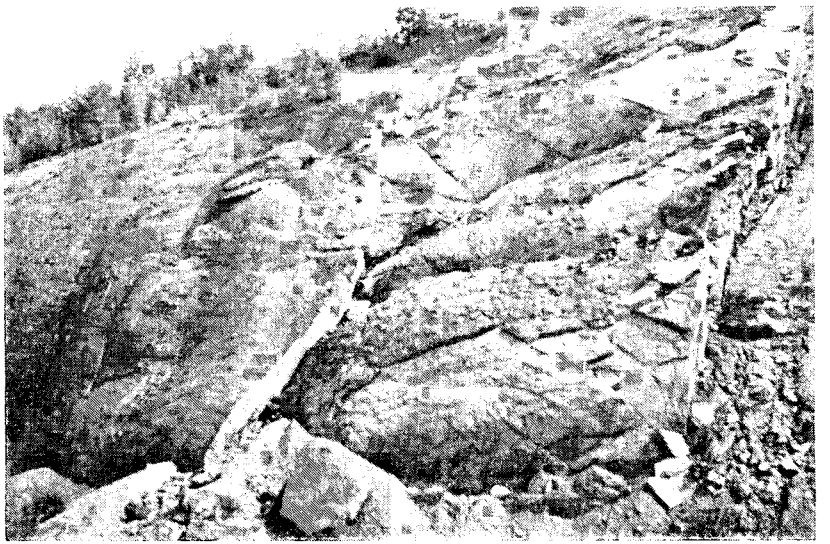

B. Conjugate wrench faults of two stage IV substages on the south wall at the southwest corner. The south-wall thrust terminates against the prominent left-lateral wrench fault in the center of the photograph.

wrench faulting had been completed before major folding. However, at several places on the whaleback anticline and high in the southeast corner of the mine, there is unequivocal evidence that some wrench faults were active during stage V folding. For example, on the transverse fault zone trending with az 30° through #1 on the crest of the whaleback anticline, the angle between slickenlines and the bedding-fault intersection viewed in the fault plane ranges from 15° to 90°, and there is evidence that smaller angles are associated with earlier faulting, larger angles with later. At the north end of the fault zone where it intersects the vertical north wall of the whaleback, slickenlines curve gradually from north plunges that meet the bedding-fault intersection at 40° to horizontal attitudes that meet at 90° (pl. 9). Left-lateral slip is indicated throughout the history of this faulting, but it began as wrench faulting while beds were being tilted to approx 45°, and it terminated as transverse extension grabens (stage VI), which grew out of stretching parallel to the fold axis as the fold continued to grow (fig. 9). The trend of the grabens follows the early wrench fault, although the mechanism of faulting has changed from the early, contractional, pre- or syn-folding wrench faulting to the late, extensional faulting.

Between #0 and #1 on the south limb of the whaleback, the same transverse fault zone through #1 shows a complex of overprinted slickenlines which may be interpreted similarly, as illustrated by figure 10, a diagram of slickenlines on the fault surface. Left-lateral wrench faulting is indicated by the nearly horizontal slickenlines that formed after fold-

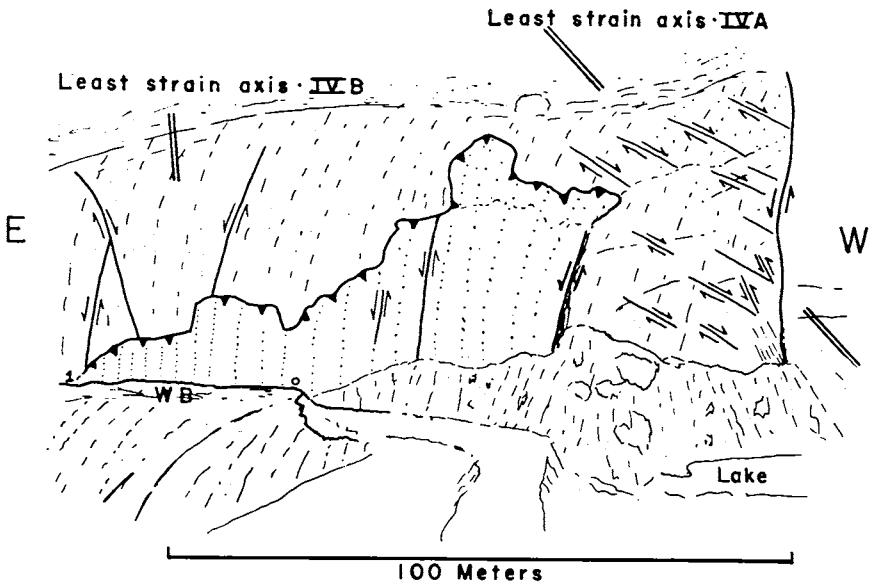

Fig. 6. Interpretive drawing of plate 1-B showing the thrust and IVA and IVB conjugate wrench-fault systems in the southwest corner.

PLATE 7
Thrusts

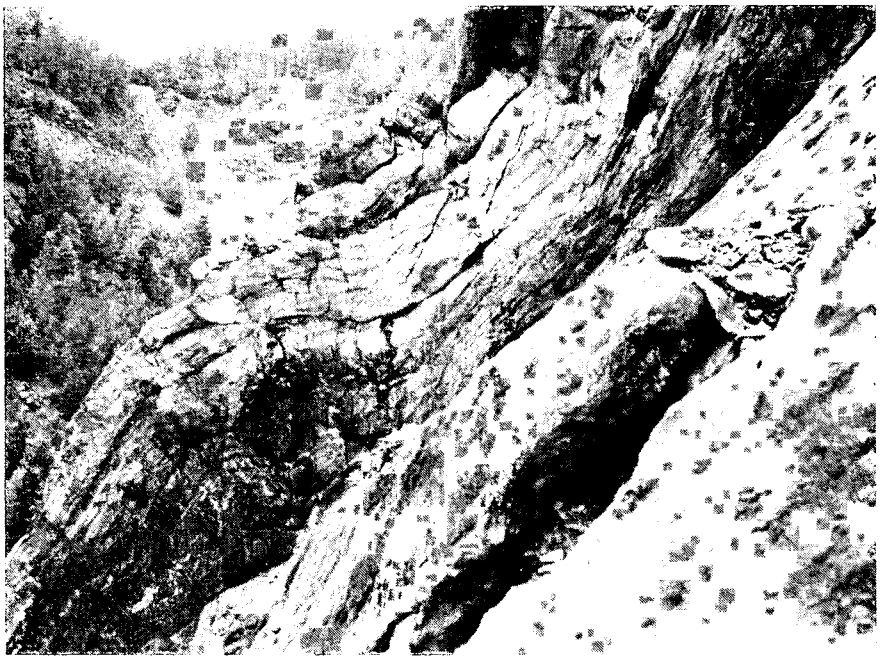

A. Intrabed wedge thrusts, photographed at the southwest corner. View looking east into the edge of the sandstone that underlies the south wall.

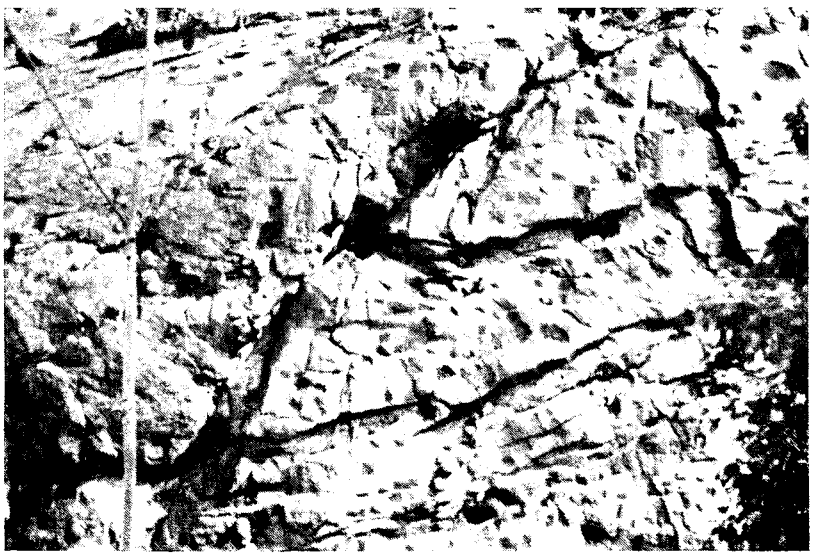

B. Stage IV thrust fault exposed on the north limb of the whaleback anticline between #3 and #4. The fault trace is not parallel to the hinge of the anticline. Fault slickenlines perpendicular to the fault trace are visible in the center of the photograph. Strike grabens of stage VI offset the fault surface.

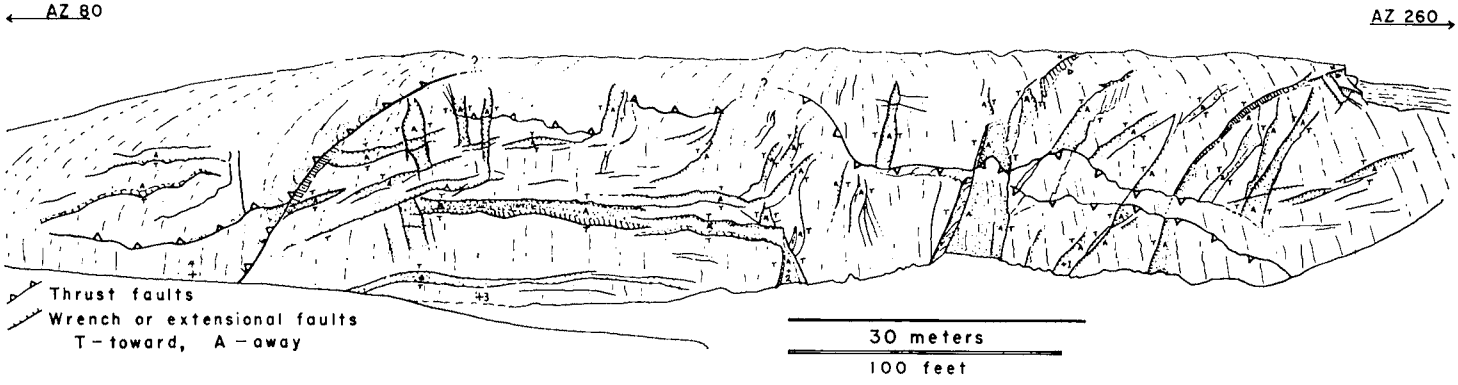

Fig. 7. Drawing of north limb of the whaleback anticline.

ing of the limb to a dip of approx 50°. Differences in the attitude of the nearly horizontal slickenlines are the result of post-slickenline bending of the beds and fault plane (fig. 10). The cross-cutting, overprinted slickenlines that meet the bedding at nearly 90° formed during extensional faulting accompanying the growth of the fold. At this end of the transverse fault zone through #1, there was apparently no continuous movement along the fault zone, athough many slickenlines curve gradually into others. Thus, at both ends of the transverse fault zone through #1, contractional left-lateral wrench faults initiated prior to or near the beginning of the stage V folding continued to grow either continuously or discontinuously throughout folding and eventually participated in the extension that occurred during the last stages of folding (stage VI).

At #2 on the north limb of the whaleback anticline, both right- and left-lateral wrench faults may be viewed in the plane of the vertical bedding (pl. 10-A). Slickenlines on the wrench faults are not exactly parallel to fault-bedding intersections, and, by interpreting slickenlines and bedding displacements, right- and left-lateral wrench faults may be differentiated. Each orientation of wrench faults is paralleled by later extension faults, which are recognized by slickenlines oriented perpendicular to the fault-bedding intersection. Thus, wrench faults that originated during earlier contraction parallel to bedding have been reacti-

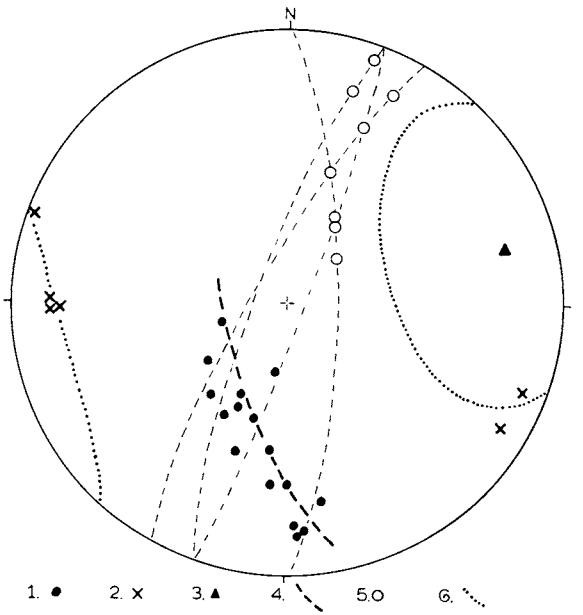

Fig. 8. Equal-area projection: structural elements in the fourth order anticline illustrated in plate 8. 1. bedding poles; 2. fault poles; 3. π-pole to bedding (fold hinge); 4. π circle through bedding poles; 5. slickenlines on fault surfaces; 6. loci of all possible wrench-fault poles intersecting the hinge at 50°, rotated around the fold hinge.

PLATE 8

Relationships of wrench faults, thrusts, and folds

A. Fourth order anticline within the north anticline between #1 and #2. A left-lateral wrench fault with slickenlines is visible to the left and below the hammer on the steep limb.

vated during later extension parallel to bedding, a conclusion also reached in the fault zone passing through #1. Reactivation of early wrench faults during later, bedding-parallel extension (stage VI) is also illustrated in plate 10-B.

In summary, this section has shown that wrench faults transverse to stage V folds originated either during bed-parallel contraction prior to folding (slickenlines rigorously parallel to fault-bedding intersections) or after beds had been folded at least 40°. Once formed, some suitably oriented faults remained active throughout stage V folding and eventually participated in stage VI extension.

Stage V: Large-scale folding.—Folds of third order (Nickelsen, 1963) are the most obvious structural features exposed in the mine (pl. 1-A). Although the syncline on the east wall (pl. 1-A) and the crest of the whaleback anticline are both concentric in profile near the hinge, there is other evidence that the folds in the mine approximate the geometry of kink-band folds that have resulted from interference between intersecting kink bands of different attitude. The limbs of the east-wall syncline have mostly been removed by erosion, but it appears that they are quite planar. The whaleback anticline is concentric only near the hinge, its limbs are nearly planar. The folds are characterized by narrow hinge zones where most bending takes place and planar limbs thus conforming to the kink-fold geometry that has been recognized throughout the Valley and Ridge Province in Pennsylvania by Faill (1969, 1973).

PLATE 8 (continued)

B. Close-up of the lower part of the folded left-lateral wrench fault shown in (A). Note slickenlines on the wrench fault and the brow of a small thrust visible on the bedding surface above the hammer.

Kink geometry is manifested best in the north anticline which changes profile from a flat-crested box fold west of the entrance road to a narrow anticlinal crest east of the entrance road. This abrupt change in profile is explained (Faill, 1972, fig. 20) by an inclination of the kink junction axis to the bedding. In the north anticline, the kink junction axis is inclined west, and the anticline plunges east, changing profile along strike as the kink junction axis climbs through the stratigraphic section. Additional evidence of kink folding is the presence of two intersecting sets of bedding slickenlines bearing 10° and 340°, which indicate directions of differential bedding slip correlated with the different kink bands and kink axes (Faill, 1972, p. 1300) making up the two limbs of the fold. Kink geometry is also demonstrated in a fourth-order fold shown in plate 8-A. It is interesting to note that recent descriptions of other foreland fold-thrust belts such as the Canadian Rockies (Dahl-

PLATE 9
Wrench-fault fold relationships

Curved slickenlines on a transverse contraction-extension fault between #1 and #2 on the north limb of the whaleback. View is toward the east. See figure 9 for interpretation.

strom, 1970) and the Swiss Jura (Laubscher, 1976) have demonstrated the importance of kink folds in these areas.

Stage VI: Fold-generated upthrusts and grabens.—Crowding in fold cores and extension in the outer arc of folds above the neutral surface of anticlines formed the last recognized stage of Alleghany orogeny. This stage occurred as a consequence of stage V folding and may have been initiated at different times in different places as folds grew. Except for the normal fault in the northwest corner, which appears to be associated with the larger upthrust depicted by Arndt, Danilchik, and Wood (1963, sheet 2, sec. D), there is no evidence of structures generated by crowding in fold cores. Extension in the outer arc above the neutral surface is very well shown by grabens in the tight whaleback anticline but does not appear in other folds, presumably because they are not exposed at the correct stratigraphic horizon. In the whaleback anticline, extension of bedding has occurred both parallel and perpendicular to

the fold hinge as shown by the transverse grabens and strike grabens (fig. 7). Transverse grabens either follow earlier wrench fault zones (pl. 10-A, -B) or are perpendicular to the hinge (fig. 7; pl. 11-B). Both strike grabens and transverse grabens following previous wrench faults are found on both limbs of the whaleback anticline, but they are most dramatically shown on the north limb (fig. 7). Strike and transverse grabens interact in several ways. In some places strike grabens terminate against transverse grabens as shown in plate 11-A. Plate 10-A shows the transverse graben in larger scale. In other places, transverse grabens perpendicular to the hinge offset strike grabens, indicating that they are slightly later (pl. 11-B). This observation plus the prevalence of transverse grabens between #2 and #3 on the north limb of the whaleback anticline (fig. 7) suggests that the last structural event may have been warping of the whaleback anticline around a vertical axis. It is also possible that stretching parallel to fold axes becomes large enough to form the transverse grabens only when the fold attains the high amplitude visible in the whaleback anticline (William Chapple, 1977, personal commun.).

Complex systems of jointing have formed as the rocks were fractured and refractured in several strain episodes during which strain axes were differently oriented. The resulting joint patterns illustrated in plate 2 are cumulative, because no joints have been erased by flow or recrystallization (Nickelsen, 1976). In addition to the joints in ironstone of stage II and the vertical left-lateral wrench fault of stage IV, plate 2-A

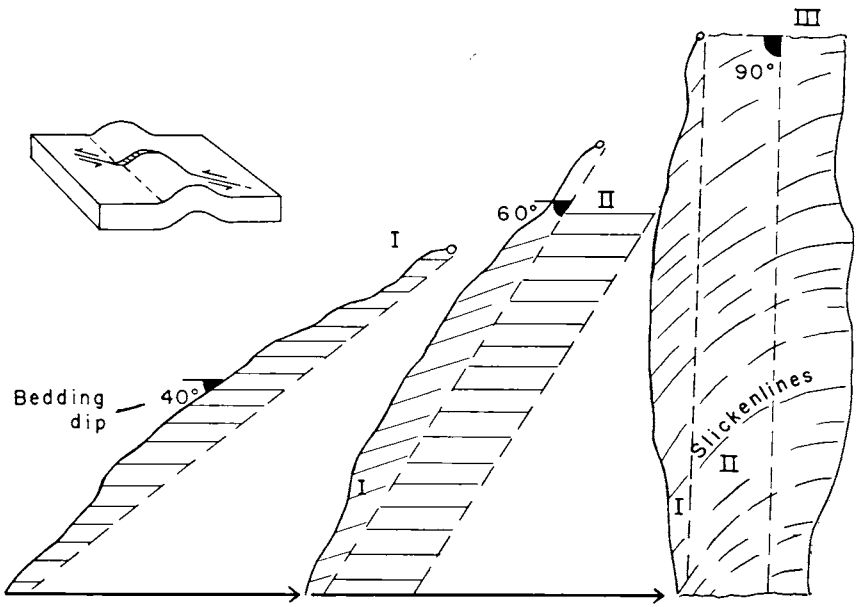

Fig. 9. Interpretation of the transverse fault illustrated in plate 9.

PLATE 10

Extension faults paralleling earlier wrench faults

A. Conjugate, contractional, stage IV right- and left-lateral wrench faults at #2 on the north limb of the whaleback define a triangular block, which later moved perpendicular to bedding during stage VI extension.

also shows a horizontal extension joint of stage VI. Stage VI joints result from extension in the outer arc of folds as is best visualized in the horizontal joints shown in plate 4. In plate 2-B the vertical stage II extension joints are overprinted by a diagonal set of quartz-filled extension joints related to the thrusting of stage IV and a horizontal set of extension joints formed in stage VI. Since the joints of each stage formed perpendicular to the greatest axis of strain, the cumulative joint patterns of plate 2 provide evidence of a 90° interchange of local strain axes between stage II and stage VI.

As described in a previous section, transverse grabens commonly follow earlier wrench fault zones, and the wrench faults either show curving slickenlines that demonstrate their continuous activity from stage IV to stage VI or overprinted slickenlines that demonstrate activity in stage IV *interrupted* and then continuing in stage VI. Interrupted

PLATE 10 (continued)

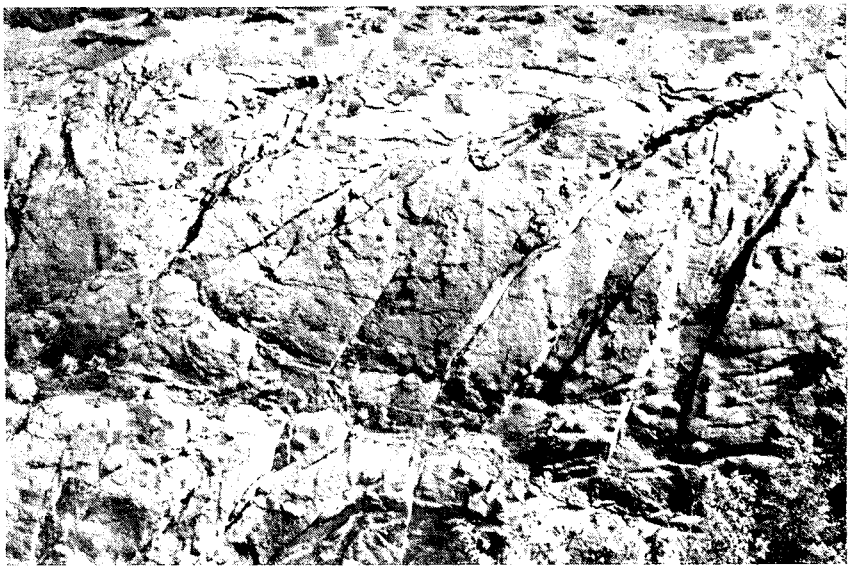

B. Stage IV conjugate wrench faults on the north limb of the whaleback between #0 and #1 that served as boundaries for stage VI grabens and horsts. The stage IV least strain axis plunges 50°-60° left, bisecting the acute angle between wrench faults. The bench in the lower third of the picture is the front of a stage IV thrust.

transverse grabens have complex histories as illustrated by one at the east end of the whaleback on the south limb (fig. 11). The fault on the right is a stage IV left-lateral wrench fault with slickenlines plunging directly down the fault plane. The fault and its slickenlines were bent by stage V folding so that, near the top of the drawing, slickenlines rake 60° south (fig. 11). Also here are overprinted slickenlines that rake 85° north. They are related to bed-parallel extension and graben formation during stage VI. The fault on the left makes up the other side of a debris-filled graben. Although they parallel the stage IV wrench fault, both this fault and the intervening graben were formed during stage VI extension parallel to the hinge of the whaleback anticline.

Three separable stages have contributed to the development of this structure: stage IV left-lateral wrench faulting, stage V folding, which has bent bedding, the wrench fault, and its slickenlines, and stage VI extension, which formed a transverse graben. Stage VI graben is bounded on the right (east) by a fault that has undergone two genetically different stages of movement and appears to have controlled the orientation and location of the graben when it formed during stage VI. The graben is bounded on the left (west) by a fault that did not form until stage VI. Here, as at a few other places in the mine, where fractures of earlier origin were correctly oriented with later strain axes they experienced renewed slip when later strain axes became active. A similarly

complex graben is visible along the wrench fault zone on the south limb of the whaleback between #0 and #1.

PRESENT ATTITUDE OF STRAIN AXES

The present attitude of one set of strain axes that resulted from deformation during stages II, III, and IV is illustrated in figure 12A. Although evidence exists, at places, for overprinting of strain axes of different orientation during stages II and IV and for rotation of stress axes during stages II and IV, only one mean set has been plotted. Structural elements that have been used to map the present attitude of strain axes are keyed on figure 12B to the numbers and letters below.

The minimum axis of the strain ellipsoid (λ_3 — heavy arrows) lies in bedding parallel to: (1) the acute bisector of stage IV wrench faults, (2) the trace of stage II extension joints, (3) the projection, on bedding, of slickenlines from stage IV thrust faults, (4) slickenlines on bedding planes near ironstone nodules. Either the maximum (λ_1) or intermediate (λ_2) axis of the strain ellipsoid (light arrows) also lies in bedding:

A. parallel to bedding-cleavage intersections,

B. parallel to small-scale cleavage folds,

C. parallel to the strike of thrusts or intrabed wedges,

D. perpendicular to stage II extension joints.

These strain axes, which can be traced on bedding planes throughout the mine (fig. 12-A), show considerable variation in orientation, which may have resulted from: (1) different strain-axis orientations at different stages in time of deformation, (2) strain axes from different domains that were not initially parallel and were then rotated around the hinges of stage V folds, (3) complex rotation of early (stage II, III, or IV) strain axes during later deformation. With few exceptions, it appears that option 3 — rotation of earlier strain axes by later episodes of strain — is the most likely interpretation of their present configuration. The large amount of rotation of early strain axes illustrated in figure 12A was not expected in an area such as the Valley and Ridge

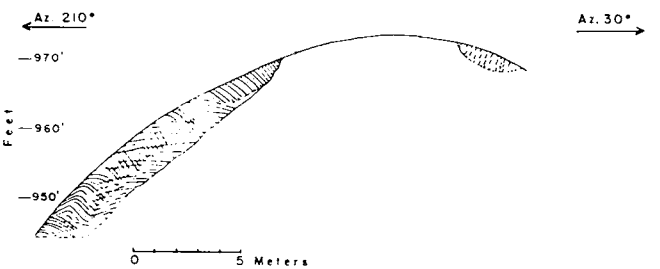

Fig. 10. Intersecting slickenlines visible on the south limb and crest of the whaleback anticline at the transverse fault through #1. View toward the west.

PLATE 11

Grabens

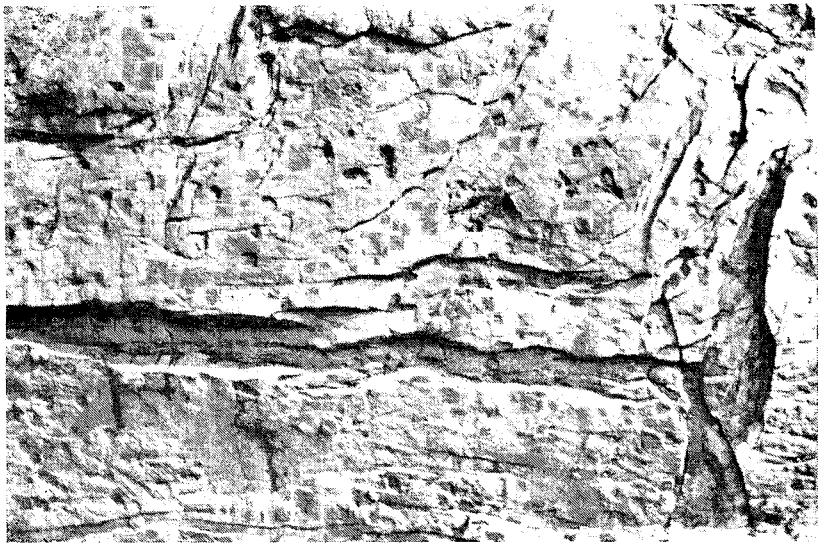

A. A strike graben on the north limb of the whaleback terminates against a transverse graben at #2.

B. Strike grabens, trending diagonally across the picture, are offset by nearly vertical transverse grabens. Photographed at #3 on the north limb of the whaleback anticline.

Province. Note particularly the bending of strain axes in the western part of the whaleback anticline and across the two limbs of the south syncline.

It is possible that, during both stage II and stage IV, stress axes rotated clockwise around a vertical axis, causing overprinting of differently oriented extension joints and conjugate wrench fault systems. Two sets of stage II extension joints, which intersect at approx 30°, have been found in all parts of the mine. Conjugate wrench-fault systems IVA and IVB have already been described from the southeast (pl. 5-A) and southwest corner (fig. 6). Both sets of intersecting structures imply that a rotation of either stress or strain axes occurred relatively early in the structural history. Since the jointing and wrench faulting, which operated at that time in horizontal beds, do not provide mechanisms for the large-scale rotation of strain axes, it is likely that stress axes rotated. Overprinting of the stage IVA conjugate wrench-fault system by the IVB system (pl. 6-B) suggests a clockwise rotation of approx 20°.

EVIDENCE OF PENETRATIVE DEFORMATION

Penetrative deformation expressed as deformed fossils and well-developed rock cleavage has been recognized at localities in the Valley and Ridge Province and Appalachian Plateau (Nickelsen, 1963, 1966, 1972; Faill and Nickelsen, 1973; Groshong, 1975; Engelder and Engelder, 1977; Faill, 1977). Additional examples of rock cleavage and deformed plant fossils that offer the potential for measuring strain are present in this mine. As in other parts of the region, penetrative deformation is

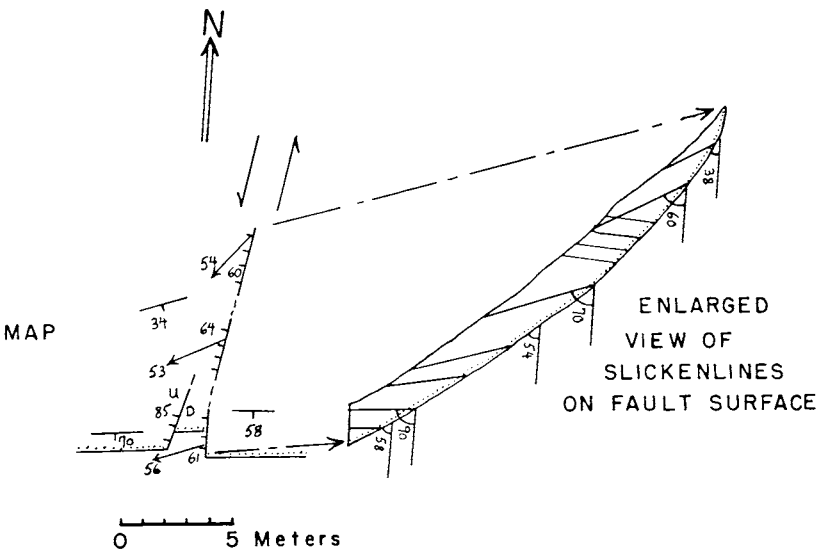

Fig. 11. Map of transverse graben at east end of whaleback anticline. Enlarged view of fault plane with slickenlines.

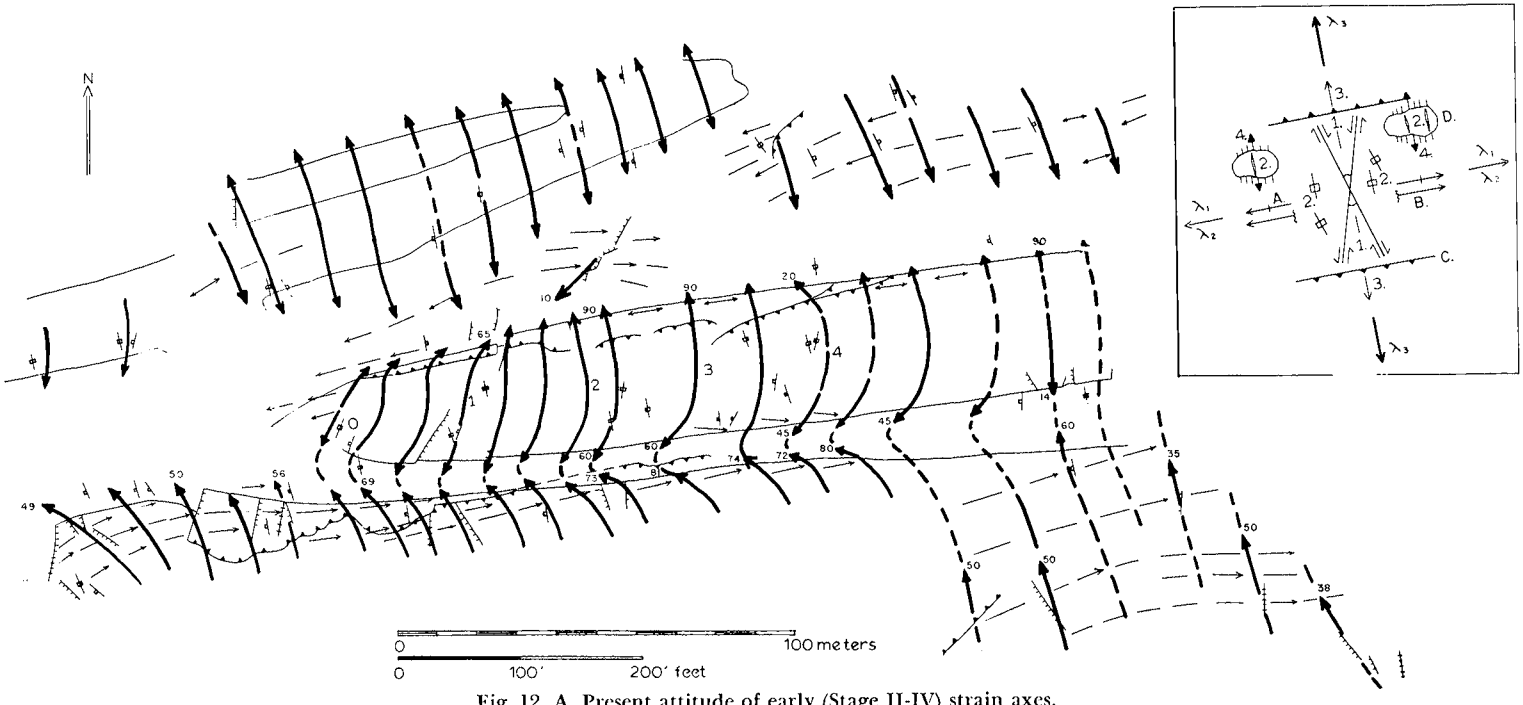

Fig. 12. A. Present attitude of early (Stage II-IV) strain axes.
B. Illustration of structural elements used to map strain axes on (A). See text for explanation.

PLATE 12
Small-scale folds

A. Small-scale folds in interbedded ironstone and shale at the southwest corner. Coin diameter is 2 cm.

recognized only in certain rock types, predominantly clay and silt shales above the coals and mudstones beneath the coals. Some thin ironstone beds are cleaved, but generally the ironstone nodules are the most competent or least ductile rocks in the sequence. Sandstones are more ductile than ironstones but less ductile than shales and mudstones. Some anthracite coal has apparently flowed from thinned limbs into thickened hinges of folds, but the amount of flowage and the mechanisms of flowage are not demonstrable here because of lack of exposure. Many pieces of anthracite occurring as float contain abundant closely-spaced, acutely intersecting, slickensided, micro-faults suggesting that flowage has occurred by pervasive shear rather than the pressure solution or crenulation recognized in other ductile rocks.

Cleavage.—Rock cleavage occurs in shales, mudstones, and ironstones at the southwest and northwest corner and in shales and sandy shales in the east wall. Also, where small thrusts cut sandstone beds, the bent sandstone above and at the front of the thrust is cleaved.

Cleavage aspect is controlled by structural position and by lithologic factors, particularly primary clay-mineral orientation, detrital quartz content, and the presence of ironstone cement. In the high strain environment at the brow of thrusts in sandstones, the cleavage intersects the thrust at less than 50° and is visible as quartz grains parallel to

PLATE 12 (continued)

B. Negative print of a thin section illustrating a class 3 fold from southwest corner. Note upward convergence of fractures, which, in part, follow crenulation cleavages. Bar = 1 cm.

the trace of cleavage on the thin section. These quartz grains are bounded on their long sides by sutured zones, enriched in clay and carbon, which result from pressure solution and residual clay accumulation (pl. 14-C).

Normally, cleavage is expressed either as crenulations of the primary, bed-parallel, clay minerals of clay shales or as clay-carbon partings (Nickelsen, 1972) resulting from pressure solution and residual accumulation of clay and carbon in silty shales or ironstones. Crenulation cleavage cutting across bedding in clay shales passes up or down section into clay-carbon partings in rock types with detrital quartz grains or chemical carbonate, thus proving their simultaneous origin. Crenulation cleavages are spaced at a frequency of 0.02 to 0.1 mm, and clay minerals on the limbs of crinkles have been rotated 40° to 60° from their original bedding attitude toward the axial plane of the crenulation cleavage. No

PLATE 13
Crenulation cleavages

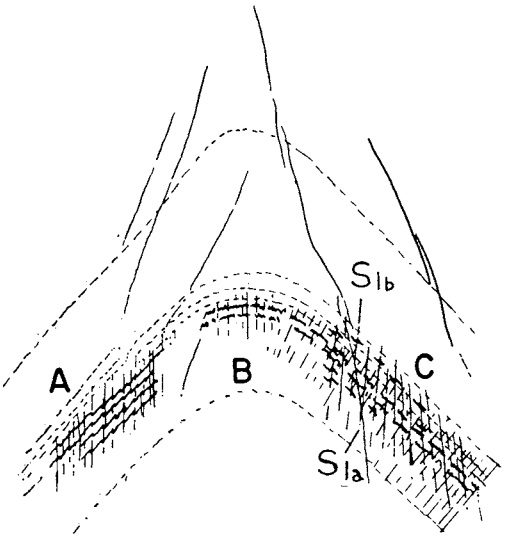

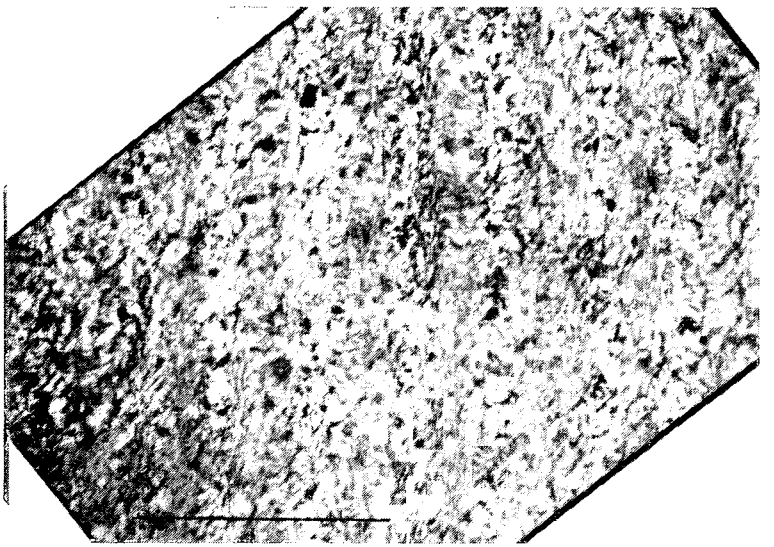

A. Z-shaped crenulations of bedding-parallel phyllosilicates on the left limb of the fold illustrated in plate 12-B. Plane light, bar = 0.25 mm.

PLATE 13 (continued)

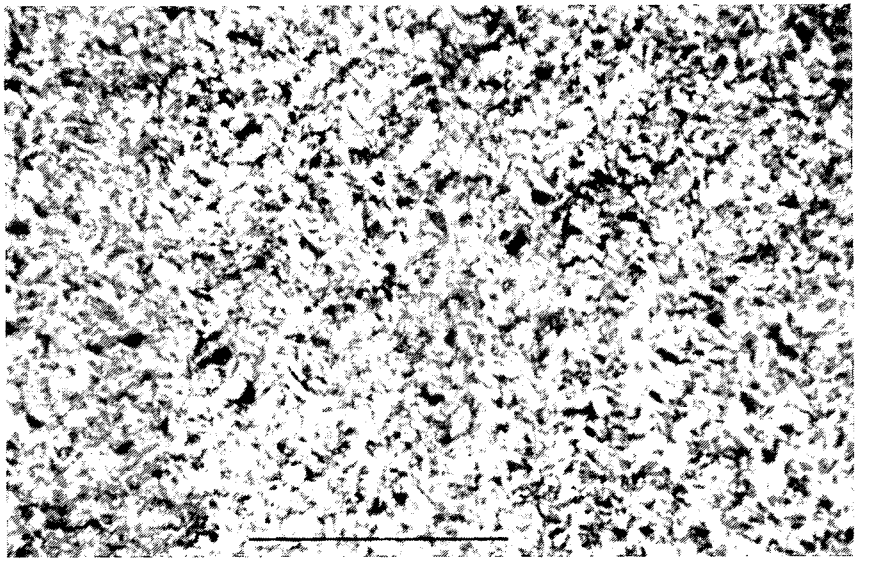

B. Symmetrical crenulations on the crest of the fold in plate 12-B, which result from bed-parallel shortening of 15 to 25 percent. Crossed nicols, bar = 0.25 mm.

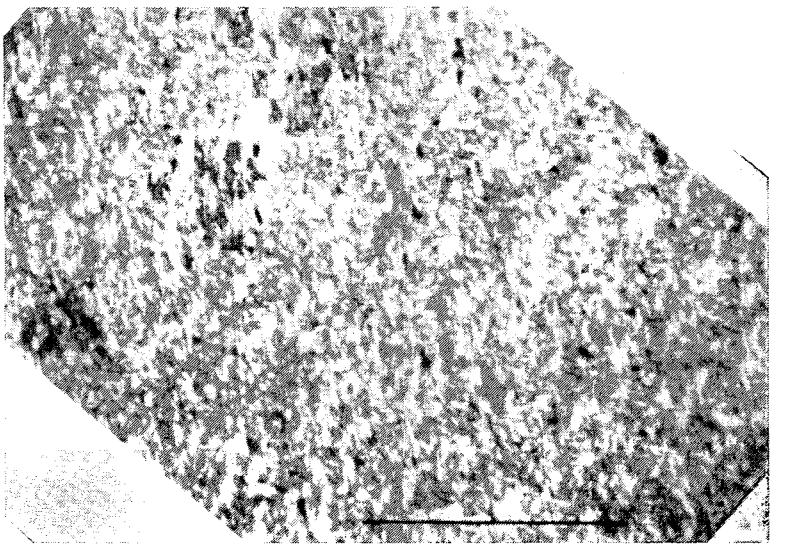

C. Two crenulation cleavages on the right limb of the fold in plate 12-B. S_{1a} is nearly perpendicular to bedding whereas S_{1b} is close to the attitude of the axial surface of the fold. Crossed nicols with gypsum and condenser, bar = 0.25 mm.

PLATE 14

Pressure-solution cleavages

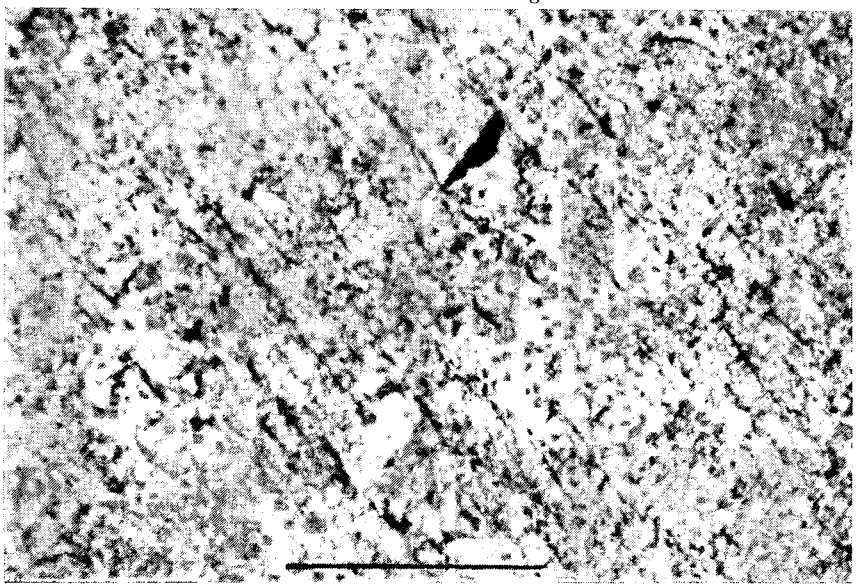

A. Spaced cleavage marked by clay-carbon partings in quartz-poor shale. Cleavage northwest-southeast, bedding northeast-southwest. Crossed nicols with condenser, bar = 0.25 mm.

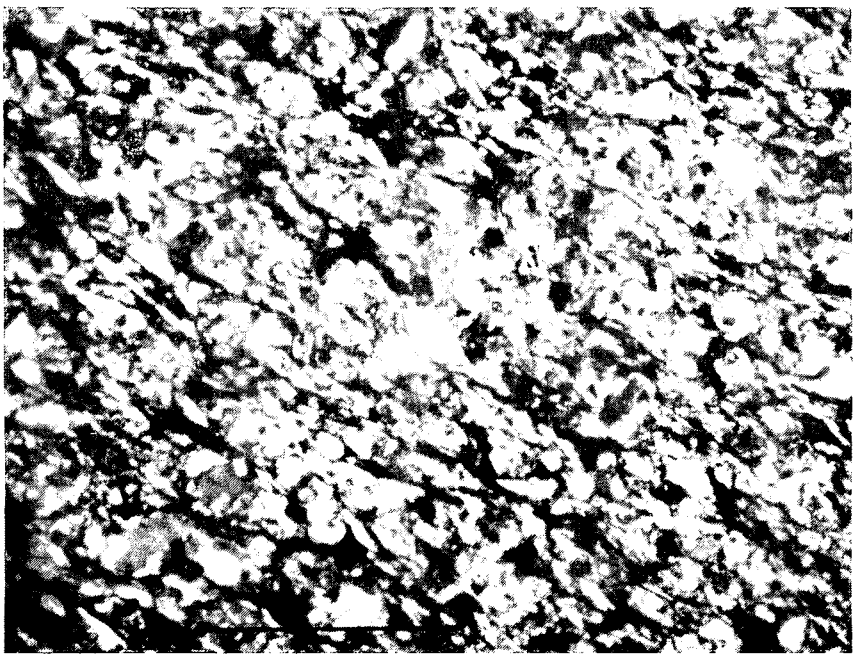

B. Spaced cleavage in quartz-rich siltstone. Clay-carbon partings are irregular, are controlled by grain boundaries, and contain parallel phyllosilicates. Cleavage northwest-southeast, bedding northeast-southwest, crossed nicols, bar = 0.25 mm.

PLATE 14 (continued)

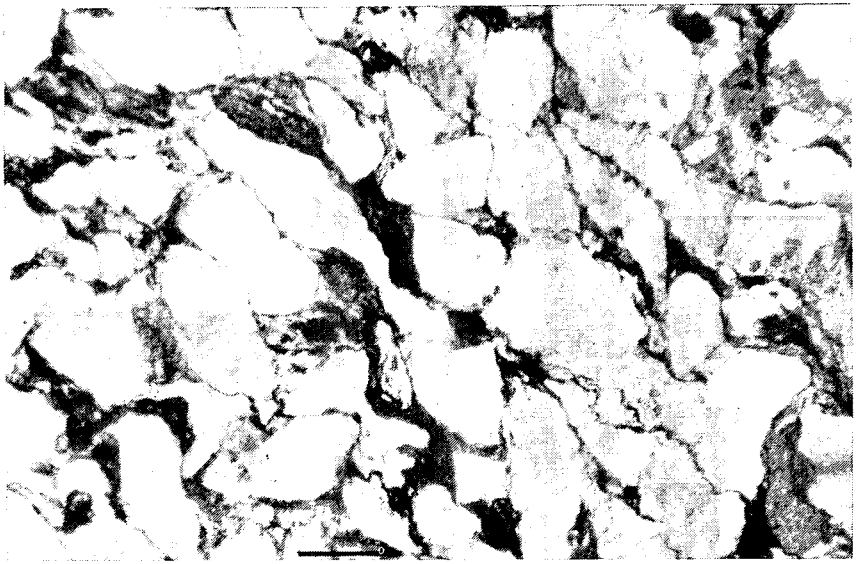

C. Spaced cleavage in sandstone at the brow of a small thrust as in plate 8B. Elongate quartz grains and clay-carbon partings formed by pressure solution. Cleavage northwest-southeast; plane light, bar = 0.25 mm.

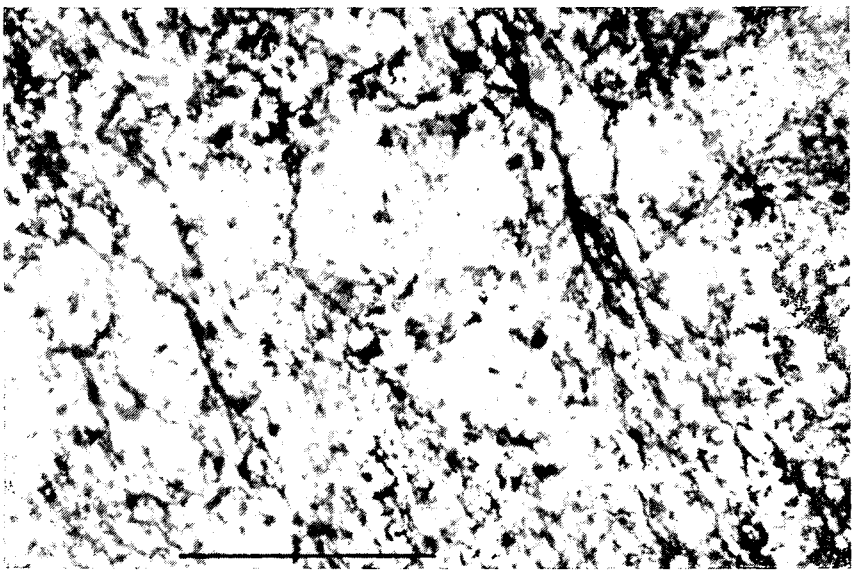

D. Spaced cleavage consisting of clay-carbon partings of different thickness and frequency in different rock types. Thick, widely-spaced clay-carbon partings in the quartzose layer diverge into many thin partings in argillaceous rock. Cleavage northwest-southeast; bedding northeast-southwest; crossed nicols with condenser, bar = 0.25 mm.

growth micas or clay minerals are present, and the transposed fabric is due completely to rotation of original bedding-parallel micas and clays toward the plane of the cleavage. The limbs of some crenulations in silty shales are emphasized by clay-carbon partings.

An excellent example of primary crenulation cleavage in a clay shale that exhibits a bed-parallel preferred orientation of clay minerals was collected in the southwest corner. Here the cleavage is associated with small-scale stage III folds in interbedded clay shale and ironstone (pl. 12-A). A thin section of the hinge of one of these folds shows that it is a class 3 fold (Ramsay, 1967, p. 367), marked by diverging dip isogons and bed thickening in the hinge (pl. 12-B). Crenulation cleavage is parallel to the fold axial surface in the hinge (pl. 13-B) and on fold limbs (pl. 13-A and -C), though cleavage orientation on the two limbs results from different processes. Two crenulation cleavages are present on the right limb of the fold — an earlier cleavage S_{1a}, which has been externally rotated in a clockwise direction with bedding, and a later cleavage S_{1b}, which cuts through bedding and the earlier cleavage (pl. 13-C). The two cleavages on the right limb formed successively during stage III minor folding in the principal plane perpendicular to the least strain axis. Neither of these cleavages shows evidence of slip along cleavage planes following their definition by crenulation. Cleavage S_{1a} was passively rotated with the fold limb but did not participate in the folding process. In contrast, the single crenulation cleavage on the left limb has undergone right lateral shear, which has caused clockwise rotation of the cleavage, opposite to the counterclockwise external rotation of the fold limb. Only one cleavage occurs on the left limb of the fold, because this cleavage has actively rotated during folding, incrementing strain throughout the process.

Clay-carbon partings, which are the cleavage in silty shales, are spaced at 0.01 to 0.05 mm but coalesce, diverge, and anastomose through the rock, generally being more closely spaced at points of strain concentration (pl. 14-A, -B). Cleavage in the silty shale of plate 14-B parallels elongated quartz grains and appears to bisect the acute angle (30°) between two planes of carbon and mica concentration. That clay-carbon partings are planes of pressure solution of quartz or iron carbonate and simultaneous residual accumulation of clay and carbon is proved by embayed, elongated, quartz grains, by concentration and orientation of residual clay, large detrital micas, and carbon, and by the great similarity of the partings in these rocks to those in Silurian and Devonian limestones where partial removal of fossils against clay-carbon partings can be documented (Nickelsen, 1973). Between clay-carbon partings the original sedimentary fabric of the rock is either undisturbed or shows evidence of uncompleted kinking of phyllosilicates toward the plane of the cleavage. The rock is composed of domains where sedimentary fabric is little disturbed alternating with domains where platy minerals are aligned parallel to cleavage (pl. 14-A). Thus, the cleavage does not penetrate completely the rock fabric, although in the field at the hinges of

some folds the rock looks like slate. The most appropriate field term for this cleavage is spaced cleavage, but it takes different forms in different rock types when viewed under the microscope. In the field it is impossible to differentiate clay-carbon parting cleavage from primary crenulation cleavage.

In all rock types the cleavage seems to parallel the principal plane perpendicular to the least strain axis. Different cleavage aspects are a consequence of the dominant process — pressure solution or crenulation — that produces the strain in the rock. Thus, in shales rich in well-oriented phyllosilicates, crenulation cleavage is well developed, whereas in silty shales and ironstones, pressure solution of quartz and iron carbonates yields clay-carbon partings enriched in insoluble phyllosilicates and carbon. In such rocks, loss of framework support may lead to rotation of individual residual phyllosilicates into the plane of the cleavage as described by Williams (1972) and illustrated in plate 14. By comparing the length of the fold trains of cleavage crenulations with their unfolded length, I have estimated that the crenulation cleavage (pl. 13-B) resulted from bed-parallel shortening of 15 to 25 percent at the hinge of the fold shown in plate 12-B, clearly only a minimum estimate of the total shortening present.

Assuming no extension parallel to the hinges of crenulations, the bed-parallel shortening associated with crenulations yields ratios of principal elongations viewed in bedding of 0.75 to 0.85. Cleavage started perpendicular to bedding and has been rotated externally with bedding, so that it diverges upward on anticlines and converges upward in synclines. In addition, internal rotation on the limbs of folds has rotated

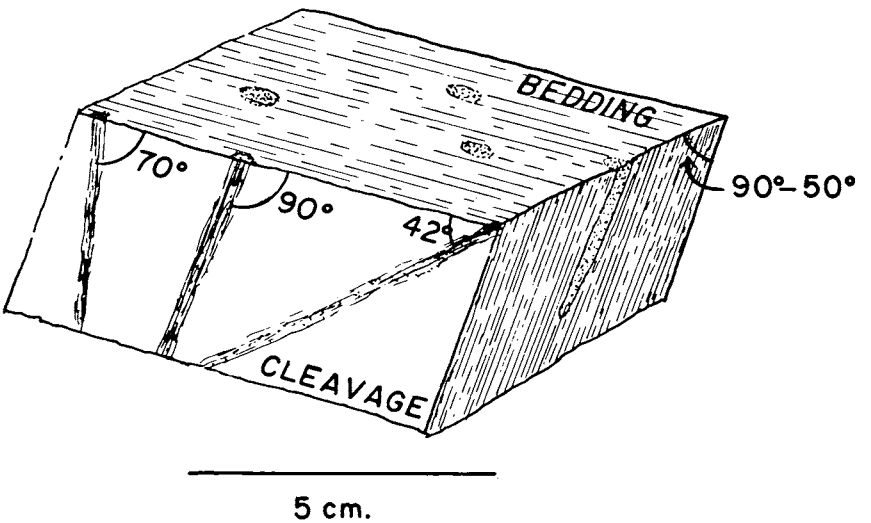

Fig. 13. Schematic drawing summarizing relations between bedding, cleavage, and organic borings in shales and siltstones of the east wall.

cleavage in the opposite sense toward axial surfaces, with the result that the angle between cleavage and bedding varies from 90° in the hinge area to 50° on fold limbs. These relations are best seen in shales and siltstones on the east wall, where silt-filled organic burrows are also visible in association with cleavage. The organic burrows are of interest, because many lie in the cleavage plane and have been rotated toward the axial plane of folds together with the cleavage. However, not all organic burrows were initially oriented perpendicular to bedding as proven by burrows, viewed in the plane of spaced cleavage, that intersect bedding at 42° to 90°[3]. Also, when viewed in the plane perpendicular to cleavage and bedding, organic burrows may either parallel cleavage or intersect it at a small acute angle, with the cleavage bisecting the distribution of visible burrows. Relations between cleavage, bedding, and organic burrows as observed in the east wall are summarized in figure 13. Both spaced cleavage and organic burrows have been rotated toward the axial plane of folds, but the angle between cleavage and bedding is the best measure of the strain involved because organic burrows were not rigorously perpendicular to bedding before deformation.

Strain determinations.—The ratio of principal elongations $\sqrt{\lambda_3}/\lambda_1$ or λ_2 in two dimensions on a bedding plane has been determined from measurements of a deformed fossil plant root or stigmaria in the mudstone beneath the coal. The original nearly right angle (fig. 14A) between the main root and its branching rootlets has been reduced by strain associated with the formation of rock cleavage. The trace of cleavage presently passes through the acute angle between the main root stem and rootlets and is assumed to parallel a principal axis of strain (fig. 14B). Figure 15, in the plane of the north-dipping bedding, shows the measurements and relationships used in computing strain: the orientation of stigmaria stem and rootlets above and below the stem; the trace of cleavage on bedding; the attitudes of conjugate wrench faults, which are later than rock cleavage because they distort cleavage. The angle between the stigmaria stem and rootlets ranges from 47° to 84°. All rootlets have been rotated clockwise, but those below the stem have generally been rotated less than those above the stem, indicating inhomogeneity of strain (fig. 14B). Both the group of rootlets above the stem and the group below the stem range through 25° in orientation, and this can be accounted for by original departures from a right angle between the stem and rootlets (fig. 14A). The ratio of principal elongations in the bedding plane was determined graphically for each rootlet-stem angle, using the chart of Breddin (1956) published as figure 5-56 (Ramsay, 1967). Angles and the ratios of principal elongations are given in table 2. The ratio of principal elongations ranges from 0.43 to 0.62 (mean 0.51) above the stem to 0.555 to 0.855 (mean 0.66) below the stem. Rock cleavage in the mudstone above the stem appears better developed than below the stem (fig. 14B), and better

[3] Angles measured between bedding and borings were 42°, 69°, 70°, 71°, 71°, 78°, 82°, 82°, 84°, 90°.

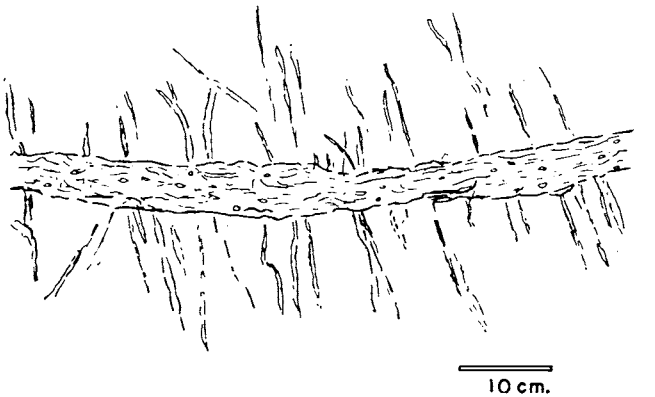

Fig. 14. A. Undeformed plant root (stigmaria) in sandstone to show dominant angles of approx 90° between stem and rootlets.

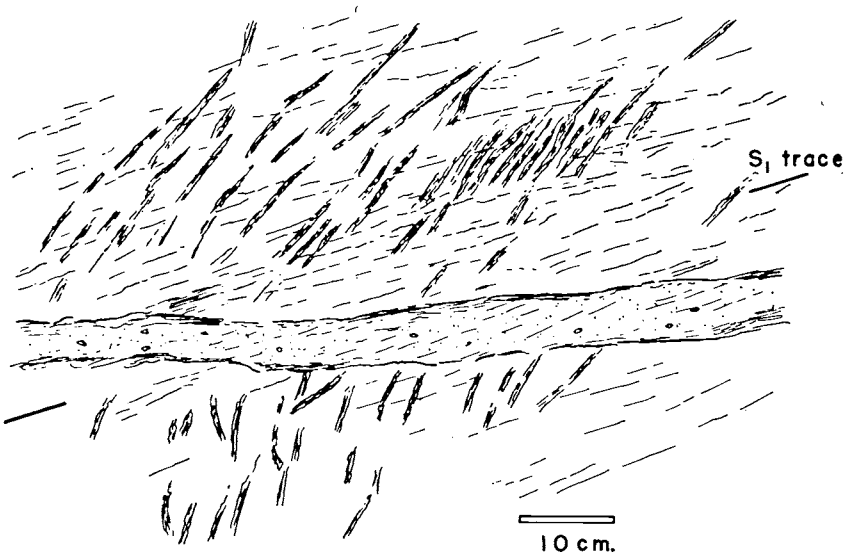

B. Deformed plant root in mudstone used to determine principal elongations in bedding plane (fig. 15 is a plot of angular relations, table 2 summarizes measurements and elongations). Rootlets above the stem show more rotation and greater strain than those below stem. The trace of cleavage intersects the stem at 20° and lies in the acute angle between the stem and rootlets.

cleavage is correlated with higher strain values. The rock is too friable to sample and prepare a thin section, so it is not possible to correlate differing strain with type or perfection of cleavage.

Figure 15 also includes conjugate wrench faults (stage IV), which distort rock cleavage (stage III). The acute bisector of the wrench faults is rotated 16° clockwise from the perpendicular to cleavage. These observations provide additional evidence that cleavage was initiated before wrench faulting and that strain axes (perhaps stress axes) rotated during successive stages of deformation. Another strain marker of less certain value is a lycopsid tree trunk, which was buried in an upright position by approx 1.5 m of beds (fig. 16A). The attitude of the tree trunk has been changed by bedding plane slip and by flattening perpendicular to rock cleavage, but the relative importance of these two mechanisms is unknown. A section of the tree viewed approximately perpendicular to its axis is elliptical (ratio 0.508) and elongated parallel to the bedding-cleavage intersection. The orientation of axes and the axial ratio observed are very similar to those observed in mud-crack polygons in other stratigraphic units of central Pennsylvania (Nickelsen, 1974). Figure 16B shows the true angular relations of bedding, cleavage, and the long dimension of the tree; angles on 16A, a drawing from a photograph, are somewhat distorted.

SUMMARY

The progressive deformation of Pennsylvanian-age rocks in the Bear Valley Strip Mine occurred during one pre-Alleghany stage and five, later, overlapping stages associated with the Alleghany Orogeny. Later structural elements have been superimposed on structures formed during earlier stages, resulting in their deformation and rotation. Extension joints formed first in horizontal beds (stages I and II) and were offset by pressure solution associated with the formation of rock cleavage during stage III. Rock cleavage is an expression of penetrative strain, which can

TABLE 2

ψ	$\phi = 90 - \theta - \psi$	$\sqrt{\lambda_3/\lambda_1}$ or λ_2
Above the Stem		
43	27	0.43
40 (2)	30	0.46
36	34	0.50
35	35	0.51
27 (2)	43	0.58
23	47	0.62
Below the Stem		
30	40	0.555
29	41	0.56
25	45	0.605
23	47	0.62
20 (2)	50	0.655
17	53	0.69
14 (2)	56	0.73
2	64	0.855

be measured in deformed plant fossils. Assuming that cleavage lies in a principal plane, such measurements have yielded mean value ratios of principal elongations in two dimensions on bedding planes from 0.51 to 0.66. Stage IV systems of conjugate wrench and thrust faults were initiated while bedding was horizontal and resulting in bed-parallel contraction. Rock cleavage in mudstones and shales is dragged against wrench faults thus proving that it was initiated before stage IV faulting. In sandstones, rock cleavage is present only in the high strain environment at the brow of thrust faults, suggesting that it was coeval with thrusting. Two overprinted conjugate systems of wrench faults (stages IVA and IVB) visible on the south wall (fig. 6) suggest that stress axes rotated clockwise 20° during stage IV. Clockwise rotation of stress axes is suggested also by the angle between the perpendicular to stage III cleavage and the acute bisector of stage IV wrench faults, shown in figure 15. Stage V kink-band folds rotated all previous structures around a hinge not necessarily parallel to previous strain axes. Some wrench faults initiated during stage IV remained active throughout stage V folding, as indicated by curving slickenlines, which can be correlated with gradually increasing bedding dips throughout the growth of the large folds. Bed-parallel, stage VI, extension in the outer arc of folds

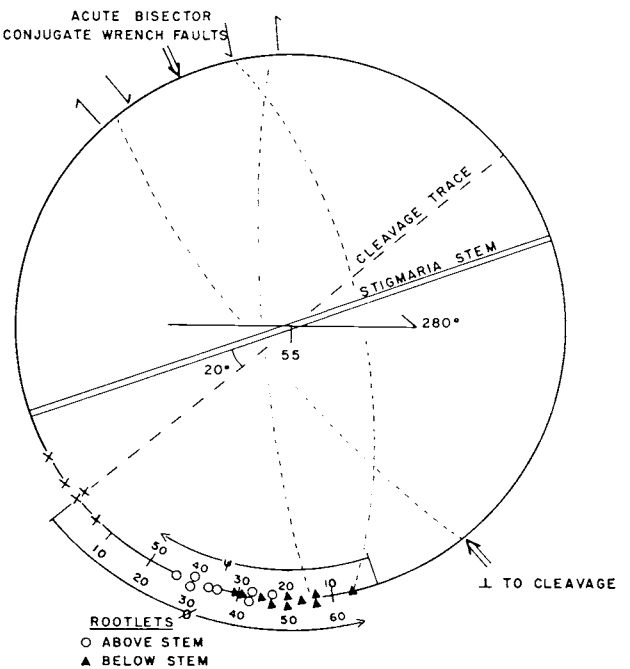

Fig. 15. Equal-area projection in the plane of bedding, of deformed stigmaria of figure 14. Figure shows angles between stem, rootlets, and cleavage trace used to compute strain (table 2). Traces of later, stage IV conjugate wrench faults, which deform cleavage, are also shown.

resulted in strike grabens and transverse grabens that displaced all previous structures. Strain axes during stages II, III, and IV were greatly distorted by stage V folding (fig. 12). Stages of deformation were not distinct, separate, events but overlapped in relative time as shown in figure 17.

Some structural elements were active during only one stage of the orogeny, whereas others remained active throughout several stages. Joints that originated early (stage I and II) were passively rotated through angles of as much as 90° during stages IV and V. But new extension joints formed in different orientations during stage IV faulting and stage V folding, resulting in the cumulative joint patterns illustrated in plate 2. Rock cleavage and small-scale folds, which originated in horizontal beds during stage III, were dragged against stage IV wrench faults and thrust faults. In places, cleavage remained active into stage V folding, as it was rotated away from its initial bedding-normal attitude. Most stage IV wrench and thrust faults were surprisingly inactive during stage V folding, probably because stage V strain axes were not parallel to stage IV strain axes (fig. 4). On the south wall, in particular, wrench faults were passively bent through > 80° without undergoing renewed slip. The fourth order fold illustrated in plate 8 and figure 8 also demonstrates passive bending of wrench faults. However, some wrench

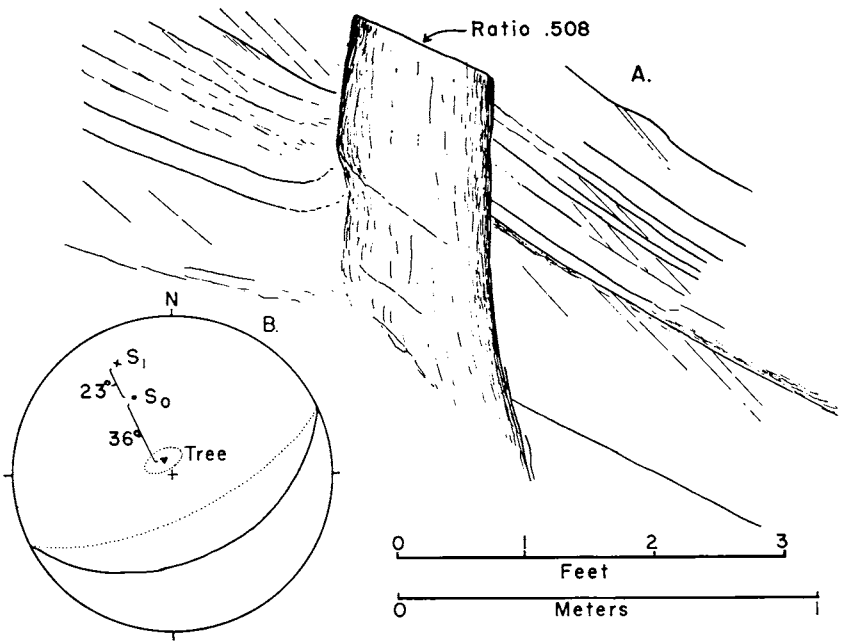

Fig. 16. A. Drawing of a lycopsid tree trunk, bedding, and cleavage from the northwest corner.

B. Equal-area projection showing angular relations between bedding, cleavage, and the elliptical axis of the lycopsid tree trunk.

faults on the whaleback anticline, which became appropriately oriented with later strain axes, remained active throughout the period from their initiation as contractional faults in stage IV until stage VI, when they served as loci for bedding-parallel extension.

Different deformation mechanisms dominated at different times throughout the orogeny, and this fact, plus rotation of early strain axes and overprinting by later stress of different orientation, has led to the recognition of the six stages. It is probable that the different deformation mechanisms operated sequentially, because various environmental parameters were gradually changing in relative importance, orientation, or magnitude. The exact nature of these changes is unknown, but the following sequence is suggested.

Stage I extension jointing occurred under relatively high pore pressure and low stress difference, the only unique stress axis being the least principal stress axis oriented perpendicular to joints and parallel to bedding. Stage II extension jointing reflects the inception of layer-parallel shortening and horizontal northwest-southwest orientation of the greatest principal stress axis, under relatively high pore pressure. Stage III pressure-solution cleavage marks the beginning of tectonic expulsion of water and local volume reductions of up to 50 percent. Crenulation cleavage in adjacent, well-bedded rocks records layer-parallel shortening of 25 percent and the inception of small-scale buckling under increasing stress difference. Stage IV shear fractures, expressed as either conjugate wrench faults or thrust (wedge) faults, probably record increasing stress difference and the resultant intersection between the failure envelope and Mohr's circle in the shear fracture region. It is impossible to estimate whether the critical factor in initiating shear failure is changes in rock parameters (changing strength due to diagenesis, porosity changes, or packing changes) or changes in environmental parameters (changing pore pressure, stress difference, or con-

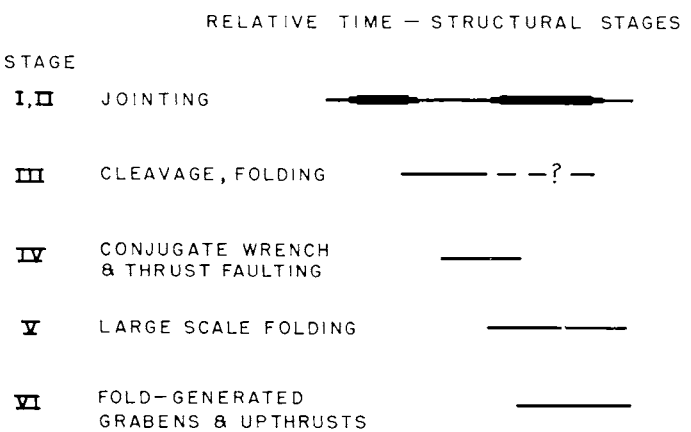

Fig. 17. Relative time of initiation and continuing activity of overlapping structural stages, Bear Valley Strip Mine.

fining pressure influenced by tectonic loading), but both may be important. Stage V large-scale buckling followed the layer-parallel shortening of stages II, III, and IV as predicted theoretically by Sherwin and Chapple (1968) and experimentally by Huddleston (1973). No general changes in environmental parameters are envisioned during either stage V or the associated stage VI.

ACKNOWLEDGMENTS

I wish to thank the many students and colleagues who have criticized and contributed to the evolution of my structural analysis of the Bear Valley Mine through more than 17 years of visits. Special thanks go to William Chapple and Rodger Faill for evaluation of an early draft of this paper and to Alvis Lisenbee for his help in initiating the detailed mapping. Also, for services rendered or ideas shared, I thank Edward Cotter, Richard Groshong, Jody Maddox, Abigail Nickelsen, Bruce Nickelsen, William Perry, Robert Scholten, and Russell Wheeler.

REFERENCES

Arndt, H. H., Danilchik, W., and Wood, G. H., Jr., 1963, Geology of anthracite in the western part of the Shamokin quadrangle, Northumberland County, Pennsylvania: U.S. Geol. Survey Coal Inv. Map C-47, Sheets 1 and 2.

Arndt, H. H., and Wood, G. H., Jr., 1960, Late Paleozoic orogeny in eastern Pennsylvania consists of five progressive stages: U.S. Geol. Survey Prof. Paper 400-B, p. B182-B184.

Arndt, H. H., Wood, G. H., Jr., and Schryver, R. F., 1973, Geologic map of the south half of the Shamokin quadrangle, Northumberland and Columbia Counties, Pennsylvania: U.S. Geol. Survey Misc. Geol. Inv. Map 1-734.

Breddin, H., 1956, Die tektonische deformation der fossilien in Rheinischen Schiefergebirge: Deutsche Geol. Gesell. Zeitschr., v. 106, p. 227-305.

Cloos, Ernst, 1961, Bedding slips, wedges and folding in layered sequences: Soc. Géol. Finlande Bull., v. 33, p. 105-122.

Dahlstrom, C. D. A., 1970, Structural geology in the eastern margin of the Canadian Rocky Mountains: Canadian Petroleum Geology Bull., v. 18, p. 332-406.

Engelder, T., and Engelder, Richard, 1977, Fossil distortion and decollement tectonics of the Appalachian Plateau: Geology, v. 5, p. 457-460.

Faill, R. T., 1969, Kink band structures in the Valley and Ridge province, central Pennsylvania: Geol. Soc. America Bull., v. 80, p. 2539-2550.

———— 1973, Kink band folding, Valley and Ridge province, Pennsylvania: Geol. Soc. America Bull., v. 84, p. 1289-1314.

———— 1977, Fossil distortion, Valley and Ridge province, Pennsylvania: Geol. Soc. America Abs. with Programs, v. 9, p. 262-263.

Faill, R. T., and Nickelsen, R. P., 1973, Structural geology *in* Faill, R. T., and others, eds. Structure and Silurian and Devonian stratigraphy of the Valley and Ridge province in central Pennsylvania, *in* Guidebook for the 38th Annual Field Conference of Pennsylvania Geologists, October 5-6, 1973: Harrisburg, Pa., Bur. Topog. and Geol. Survey, p. 9-38.

Fleuty, M. J., 1975, Slickensides and slickenlines: Geol. Mag., v. 112, p. 319-322.

Geiser, P. A., 1974, Cleavage in some sedimentary rocks of the central Valley and Ridge province, Maryland: Geol. Soc. America Bull., v. 85, p. 1399-1412.

Groshong, R. H., 1975, Strain, fractures, and pressure solution in natural single-layer folds: Geol. Soc. America Bull., v. 86, p. 1363-1376.

Gwinn, V. E., 1964, Thin-skinned tectonics in the Plateau and northwestern Valley and Ridge province of the central Appalachians: Geol. Soc. America Bull., v. 75, p. 863-900.

———— 1970, Kinematic patterns and estimates of lateral shortening, Valley and Ridge and Great Valley provinces, central Appalachians, south-central Pennsylvania, *in* Fisher, G. W., Pettijohn, F. J., Reed, J. C., Jr., and Weaver, K. N., eds. Studies of Appalachian geology, central and southern: New York, Intersci. Publishers, p. 127-146.

Huddleston, P. J., 1973, An analysis of "single-layer" folds developed experimentally in viscous media: Tectonophysics, v. 16, p. 189-214.

Laubscher, H. P., 1976, Geometrical adjustments during rotation of a Jura fold limb: Tectonophysics, v. 36, p. 347-365.

Nickelsen, R. P., 1963, Fold patterns and continuous deformation mechanisms of the central Pennsylvania folded Appalachians, p. 13-29 *in* Pittsburgh Geol. Soc., Guidebook to Tectonics and Cambro-Ordovician stratigraphy, central Appalachians of Pennsylvania September 1963: p. 13-29.

———— 1966, Fossil distortion and penetrative rock deformation in the Appalachian Plateau, Pennsylvania: Jour. Geology, v. 74, p. 924-931.

———— 1972, Attributes of rock cleavage in some mudstones and limestones of the Valley and Ridge province of Pennsylvania: Pennsylvania Acad. Sci. Proc., v. 46, p. 107-112.

———— 1974, Origin of cleavage and distorted mudcrack polygons: Geol. Soc. America Abs. with Programs, v. 5, p. 59.

———— 1976, Early jointing and cumulative fracture patterns, *in* Proc. of the 1st Internat. Conf. on the New Basement Tectonics: Utah Geol. Assoc. Pub. #5, p. 193-199.

Nickelsen, R. P., and Hough, V. N. D., 1967, Jointing in the Appalachian Plateau of Pennsylvania: Geol. Soc. America Bull., v. 78, p. 609-630.

Perry, W. J., 1975, Tectonics of the western Valley and Ridge fold belt, Pendleton County, West Virginia — A Summary Report: U.S. Geol. Survey, Jour. Research, v. 3, no. 5, p. 583-588.

Pettijohn, F. J., Potter, P. E., and Siever, R., 1972, Sand and sandstones: New York, Heidelberg, Berlin, Springer-Verlag, 618 p.

———— 1975, Sedimentary rocks, 3d ed.: New York, Harper and Row, 628 p.

Ramsay, J. G., 1967, Folding and fracturing of rocks: New York, McGraw-Hill, 568 p.

Rodgers, John, 1970, The tectonics of the Appalachians: Wiley-Intersci., New York, 271 p.

Sherwin, Jo-Ann, and Chapple, W. M., 1968, Wavelengths of single-layer folds: A comparison between theory and observations: Am. Jour. Sci., v. 266, p. 167-179.

Williams, E. G., and Bragonier, W. A., 1974, Controls of early Pennsylvanian sedimentation in western Pennsylvania, *in* Briggs, G., ed., Carboniferous of the southeastern United States: Geol. Soc. America Spec. Paper 148, p. 135-152.

Williams, P. F., 1972, Development of metamorphic layering and cleavage in low-grade metamorphic rocks at Bermagui, Australia: Am. Jour. Sci., v. 272, p. 1-47.

Wood, G. H., Jr., Arndt, H. H., and Carter, M. D., 1969, Systematic jointing in the western part of the anthracite region of eastern Pennsylvania: U.S. Geol. Survey Bull., v. 1271-D, p. D1-D16.

Wood, G. H., and Bergin, M. J., 1970, Structural controls of the anthracite region, Pennsylvania, *in* Fisher, G. W., Pettijohn, F. J., Reed, J. C., Jr., and Weaver, K. N., eds. Studies of Appalachian geology central and southern: New York Intersci. Publishers, p. 147-160.

Wood, G. H., Jr., Trexler, J. P., and Kehn, T. M., 1969, Geology of the west-central part of the southern anthracite field and adjoining areas, Pennsylvania: U.S. Geol. Survey Prof. Paper 602, 150 p.